universität wien

# MASTERARBEIT / MASTER'S THESIS

Titel der Masterarbeit / Title of the Master's Thesis

„Charged nanocellulose filters for water treatment“

verfasst von / submitted by

Khatanbaatar Byambatsogt

angestrebter akademischer Grad / in partial fulfilment of the requirements for the degree of

Master of Science (MSc)

Wien, 2022 / Vienna, 2022

| | |
|---|---|
| Studienkennzahl lt. Studienblatt / degree programmecodeas it appears on the student record sheet: | A 066 862 |
| Studienrichtung lt. Studienblatt / degree programme as it appears on the student record sheet: | Masterstudium Chemie |
| Betreut von / Supervisor: | Dr. Andreas Mautner |

## Acknowledgments

I would first like to thank Prof. Alexander Bismarck and Dr. Andreas Mautner for giving me the opportunity to do this research. Their enthusiasm has motivated me a lot in my research.

It is a great pleasure to acknowledge my deepest thanks and gratitude to Dr. Qixiang Jiang, whose guidance, support, encouragement and comprehensive advice has been invaluable throughout this work. His immense knowledge and plentiful experience have encouraged me in all the time of my work and daily life. Without him I would not have been able to complete this thesis.

I would also like to thank Amy Ho's guidance and advice in mechanical tests.

Finally, I would like to express my gratitude to my parents, my wife and my child. Without my parents' support, I would not have been able to study at the University of Vienna, Faculty of Chemistry. Their support is always my biggest motivation. Thank you!.

## Abstract

Water sources are contaminated by a large variety of pollutants including heavy metal ions from various sources, such as mining, industry, and agricultural activities. The increasing amount of these metal ions in water has been one of the growing environmental concerns, as they are exceedingly damaging to the environment and aquatic life as well as to animal and human health even at very low concentrations. Because of its wide range of industrial, medical, and technical applications, copper is one of the most frequently detected metal contaminants in the environment, particularly in water. Moreover, numerous industries, including mining, paper, petroleum, and metallurgy, discharge huge amounts of effluents containing Cu(II) ions into the environment. Among the water treatment methods, such as ion exchange, sedimentation and precipitation, adsorption, preferably with biobased adsorbents, is considered as the most effective approach to purify water, particularly to remove heavy metal ions, due to its high technical applicability, selective uptake and cost efficiency, especially for low-level heavy metal treatment in water. Biomaterials, such as cellulose are attracting increasing interest as efficient adsorbent and filter materials for water treatment, as they can be derived from various biomasses. In addition, they are cost effective due to their high abundance and renewability. Nanocellulose, i.e. nano-scale cellulose (CNF), can be tailored for selective and improved interactions through a variety of chemical modifications, such as carboxylation using 2,2,6,6-tetramethylpiperidin-1-oxyl (TEMPO), thanks to its high number of surface hydroxyl groups. TEMPO-CNF coated nanocellulose filters exhibit a high number of negatively charged carboxylic ($COO^-$) functional groups, which are beneficial for the adsorption of positively charged heavy metal ions, for instance Cu(II) ions.

The purpose of this study was to determine the efficiency of flat filters carrying TEMPO-CNF as functional adsorption agent for the removal of heavy metal ions fabricated by coating and drying foamed (referred to as foam coating) and non-foamed (referred to as cast coating) TEMPO-CNF suspensions. The second major focus was to investigate efficient conditions for the regeneration of TEMPO-CNF filters and to analyse their reabsorption capacity. The performance of TEMPO-CNF filters was evaluated in terms of water permeance as well as adsorption of Cu(II) ions. It was found that the efficiency of TEMPO-CNF filters, namely adsorption and mechanical properties, was related to their coat weight. Cast coated filters exhibited a higher areic adsorption of up to 280 mg/m$^2$ for Cu(II) compared to foam coated filters (25 to 128 mg/m$^2$) due to their higher coat weight, however, foam coated filters particularly with low coat weights exhibited higher adsorption capacities of up to 52 mg/g. In addition, both types of TEMPO-CNF filters exhibited appropriate adsorption for Ca(II) ions,

allowing the filters to reduce water hardness, which is an essential factor for the quality of water. The permeance of foam and cast coated TEMPO-CNF filters was kept at about 330000 to 430000 L / $m^2$ h MPa and 100000 to 380000 L / $m^2$ h MPa at 0.2 bar, respectively. Furthermore, up to 99 % of Cu (II) was recovered from the TEMPO-CNF filters by using optimised regeneration conditions utilizing HCl. A high amount of re-adsorption of more than 70% remained for the regenerated foam and cast coated TEMPO-CNF filters demonstrating cyclability of these filters.

## Kurzfassung

Wasser ist einer der wichtigsten Rohststoffe und Grundlage für Leben auf der Erde. Aufgrund der Klimakrise, der industriellen Entwicklung und dem Bevölkerungswachstum nimmt die Belastung des Wassers und der Umwelt durch verschiedene Schadstoffe wie z.B. Schwermetalle zu. Sie werden hauptsächlich aus dem Bergbau, Abgasemissionen, Energieerzeugungsanlagen, Metallbeschichtungen und verschiedenen Industrien in Wasserläufe freigesetzt. Die Verschmutzung von Trinkwasserquellen mit Schwermetall-Ionen stellt eine ernsthafte Bedrohung für die Versorgungssicherheit mit Trinkwasser dar und ist eine Hauptursache für zunehmende Wasserknappheit, die immer mehr Länder betrifft. Schwermetalle können sich im Grundwasser sammeln, anreichern und schlussendlich über die Nahrungskette in den menschlichen Körper gelangen, wo sie Schäden an den Nieren, dem zentralen Nervensystem, und dem Immunsystem verursachen können. Die Entfernung von Schwermetallen aus Wasser stellt daher aufgrund ihrer gefährlichen Auswirkungen auf die menschliche Gesundheit und die Umwelt eine große Herausforderung für die Gesellschaft dar. Als Beispiel und Modell für die Belastung mit Schwermetallionen dient Kupfer. Kupfer wird wegen seiner hervorragenden Eigenschaften wie zum Beispiel der elektrischen und thermischen Leitfähigkeit, sowie der hohen Duktilität in vielen verschiedenen Industrien, einschließlich Bergbau, bei der Kupfer-Messing-Beschichtung, zur Papierherstellung und in der Färberei, eingesetzt, wobei Kupferionen-haltige Abwässer entstehen, wodurch Kupfer in die Umwelt eingebracht wird. Die Verwendung von Kupfer als Pflanzenschutzmittel in der Landwirtschaft ist eine der häufigsten Ursachen für erhöhte Kupferwerte in Grundwasservorkommen. Es ist besonders für Mikroorganismen wie Bakterien, Pilze und Algen sehr giftig, weil es in der Natur nicht zersetzt wird und daher in Pflanzen und Tieren angereichert wird. Daher ist es immer noch eine sehr wichtige und herausfordernde Aufgabe, unerwünschte Metallionen effektiv und tiefgreifend aus dem Wassersystem zu entfernen, um in Zukunft sauberes Trinkwasser und reinere Oberflächengewässer zu gewährleisten. Gegenwärtig sind zahlreiche physikalische und chemische Methoden zur effizienten Entfernung von Schwermetallen aus Wasser in Entwicklung und Einsatz, einschließlich chemischer Fällung, Ionenaustausch, Adsorption und elektrochemische Technologien. Diese Methoden besitzen verschiedene positive Attribute aber auch Nachteile wie hohe Kosten, niedrige Nachweisgrenzen und Effektivität. Laut kürzlich veröffentlicheten Untersuchungen stellen Nanofilter (NF) aus leicht verfügbaren und kostengünstigen Rohstoffen, wie z.B. Cellulose, ein vielversprechendes Verfahren für die effektive Entfernung organischer und anorganischer Schadstoffe aus Wasser dar. Diese Nanocellulose-basierten Filter stellen ein energieeffizientes,

billiges, biologisch abbaubares, ungiftiges und umweltfreundliches Medium für die Wasseraufbereitung dar. Cellulose kann vielseitig chemisch modifiziert und dadurch in ihren Eigenschaften verändert werden. Außerdem kann Cellulose durch mechanische oder chemische Behandlung in Cellulose-Nanofasern (CNFs) umgewandelt werden, die hervorragende Eigenschaftung für den Einsatz in der Wasserreinigung besitzen. Um die Adsorptionskapazität von unmodifizierter Nanocellulose zu erhöhen, kann eine Vielzahl von funktionellen Gruppen durch chemische oder enzymatische Modifikationen auf die Oberfläche von Nanocellulose aufgebracht werden, beispielsweise mittels Carboxylierung, Sulfonierung, Oxidation, Phosphorylierung und Veresterung. Die Einführung von Carboxylgruppen in Nanocellulose bewirkt eine hohe Adsorptionskapazität für die Entfernung von Schwermetall-Ionen wie z.B. Kupfer-Ionen aus Wasser. So können z.B. C6-OH Gruppen selektiv 2,2,6,6-Tetramethylpiperidin-1-oxyl (TEMPO)-katalysiert oxidiert werden ohne dabei die ursprüngliche Struktur und Kristallinität zu verändern.

Hauptziel dieser Arbeit war es, in pre-industriellem (Pilot-) Maßstab hergestellte Filter mit TEMPO-CNF als aktivem Adsorbent zur Entfernung von Kupfer-Ionen aus wässrigen Lösungen zu untersuchen. Die Beschichtung von Viscose Vliesen mit TEMPO-CNF erfolgte mittels Guss- oder Schaumaufbringung. Einflussgrößen wie die Grammatur (grammage) der Adsorptionsschicht auf Absorptionskapazität, Permeabilität, und mechanische Eigenschaften sollten dabei untersucht werden. Ein wichtiger Aspekt war dabei die Wiederverwendung der eingesetzten TEMPO-CNF Filter. Es wurde festgestellt, dass die Effizienz von TEMPO-CNF Filter, insbesonders die Absorptionsfähigkeit und mechanische Eigenschaften, mit der Grammatur der Beschichtung zusammenhängen. Gussbeschichtete Filter haben aufgrund ihres höheren Beschichtungsgewichts eine höhere Absorption von bis zu 280 mg/m$^2$ für Cu(II) im Vergleich zu schaumbeschichteten Filtern (25 bis 128 mg/m$^2$). Andererseits war die Adsorptionskapazität (bis zum 52 mg/g) von schaumbeschichteten Filtern mit geringem Beschichtungsgewicht höher. Bis zu 99 % Cu(II) konnten aus den TEMPO-CNF Filtern durch die Verwendung optimierter Regenerationsbedingungen mit Hilfe von HCl zurückgewonnen werden. Die regenerierten Schaum- und gussbeschichteten TEMPO-CNF Filter zeigten dabei eine hohe Reabsorption von mehr als 70 % der ursprünglichen Adsorptionskapazität. Zudem haben beide Arten Filter eine große Absorptionsfähigkeit für Ca(II) gezeigt. Das bedeutet, dass TEMPO-CNF Filter Wasserhärte reduzieren können. Die Wasserdurchlässigkeit von geschäumten und gussbeschichteten TEMPO-CNF-Filter war etwa 330.000 bis 430.000 l/m$^2$ h MPa und 100.000 bis 380.000 l/m$^2$ h MPa bei 0,2 bar, wodurch ein hoher Wasserdurchsatz für effiziente Wasserreinigung erzielt werden kann.

## Table of Contents

## 1. Introduction

Fresh water constitutes a tiny portion of the overall amount of water on earth. Although water covers approximately 70 % of the globe, a mere 2.5 % of it is fresh water including 1.75-2 % of frozen water in glaciers, ice and snow. Only 0.5-0.75 % of the total water constitutes fresh groundwater and soil moisture. The rest (97.5 %) corresponds to oceans, seas and saline groundwater [1]. This small amount of freshwater is being depleted day by day due to pollution, thus increasing the amount of contaminated water. This poses a major threat to human life and ecosystems because polluted water contains various pollutants, including heavy metals, toxic textile dyes, pesticides and oil, as well as agricultural wastes, detrimental to (human) health [2]. The majority of water pollution is caused by human activities, such as industrialisation, population growth, urbanisation, climate change and agricultural operations. Nowadays, about one billion people do not have access to safe drinking water and basic sanitation and approximately 800 000 people die every year from drinking contaminated water [3]. About 80 per cent of all wastewater is discharged into the environment without adequate treatment. As a result, it has a detrimental effect on human health, the quality of ambient freshwater resources and the ecosystem [4]. Water sources are contaminated by a large variety of pollutants, for instance heavy metal ions, which are released into the environment from mining and industrial or agricultural activities. High concentrations of heavy metals can be dangerous to animals and humans, causing severe health problems and even death in extreme cases. Therefore, purification of both potable water and wastewater, particularly the removal of heavy metal ions from water, is urgently needed in order to ensure supply of safe drinking water and decrease in global water pollution. Various approaches, including ion exchange, chemical adsorption, flocculation and biological growth are available to remove heavy metals from water, but each has its own set of disadvantages, including high energy requirements, their synthetic material content, and the generation of toxic sludge [5]. Thus, an advanced, inexpensive and environmentally friendly technology needs to be developed to address these major water treatment issues [6]. Adsorption based on natural and renewable materials is one of the most cutting-edge approaches for water purification due to its convenience, ease of use, and simplicity of construction [7].

Among the biomaterials, nanocelluloses (NC) have been shown to be potential absorbent materials appearing to be advantageous over other conventional materials and technologies for pollutant removal from water due to their excellent mechanical properties, high specific surface area and environmentally friendly production [5]. Another big advantage of NC is that it can be extracted from a variety of biomasses such as trees, plants, weeds and also agricultural side streams [8]. NC contain a multitude of hydroxyl groups (-OH) on their surface,

which can be chemically modified, for instance into carboxylic groups (-COOH), to increase the affinity towards metal ions. Carboxylic groups exhibit strong affinity towards various (heavy) metal ions, such as copper ions. 2,2,6,6-Tetramethylpiperidin-1-oxyl (TEMPO) mediated oxidation is applied as an effective method to selectively convert hydroxyl groups located at cellulose's C6 position into carboxylate groups on the surface of cellulose fibers. Nanofibrils generated therefrom are commonly denominated as TEMPO-CNF [9]. TEMPO-CNF have potential applications as environmentally friendly and bio-based nanomaterial in a variety of fields, including water treatment [10].

## 2. Theoretical background

### 2.1. Water contamination by heavy metal ions

Nowadays, the increasing amount of heavy metal ions in water has been one of the growing environmental concerns because of their high persistence and toxicity. Thus, heavy metals are one of the most dangerous contaminants in water. Heavy metals are defined as metallic chemical elements having a density of more than 5 g/cm$^3$. These include for instance nickel, copper, arsenic, mercury and cadmium, which are highly harmful to the environment and aquatic life as well as human health even at very low concentrations [11]. Heavy metals emerge into the environment by natural and anthropogenic processes. Natural sources of heavy metals include volcanic eruption, forest fires, rock weathering and wind-borne soil particles. Anthropogenic activities, such as industrial production, mining and agriculture, are a major source of heavy metal ions released into water bodies, leading to a severe environmental problem. Heavy metal pollution usually follows a cycle: industry, environment, soil, water, foods and humans (Figure 1) [12].

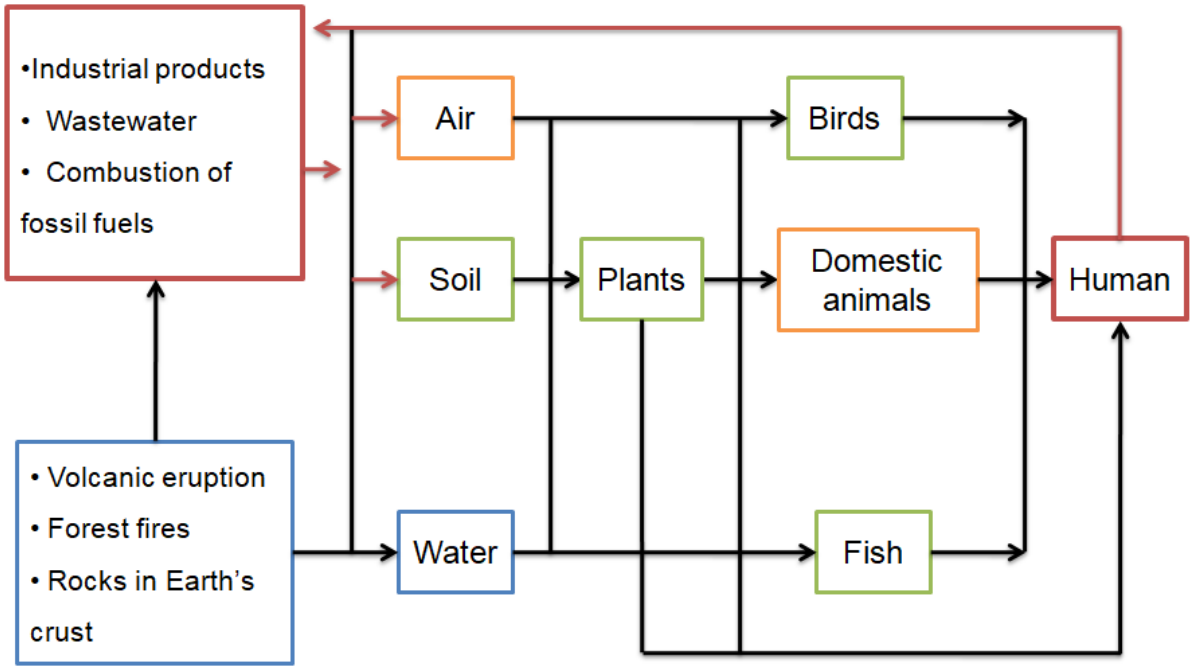


**Figure 1: Sources of heavy metals and their cycle in the environment [11].**

Heavy metals can enter human bodies through food, drinking water or air and accumulate therein leading to health threats. Heavy metal toxicity in humans and other living organisms may cause brain damage or a decrease in mental functions and central nervous system, as well as damage to the liver, lungs and other vital organs [4, 6]. Copper is among the most commonly found heavy metal contaminants in the environment, especially in water because many industries, including mining, paper, petroleum and metallurgy, release large amounts of effluents containing Cu(II) ions into the environment [13]. Copper, as a trace element, is essential in maintaining crucial processes in human function and metabolism, nevertheless, it is toxic at higher concentrations [14]. Copper removal from water, in particular industrial effluents, is important not only because of its harmful effects on the environment, but also worthwhile in order to recover and reuse copper in a variety of industrial applications. Cu(II) ions are removed from wastewater using physical, chemical and biological methods prior to being released into the environment. Among these treatment techniques, adsorption is regarded as one of the most efficient, cost-effective and environmentally sustainable methods [15].

## 2.2. Water treatment

### 2.2.1. Removal of heavy metal ions by adsorption

Several methods, including ion exchange, electrochemical treatment, sedimentation, precipitation and cationic surfactants, have been recently investigated for the development of productive technologies to reduce the amount of heavy metal ions in water and to increase the quality of water [16]. However, their application is limited, because the majority of them require a significant financial investment [17]. Therefore, there is pressing demand for innovative technologies, which are low cost, energy efficient and require little maintenance [18]. Among the water treatment methods mentioned, adsorption is considered as the most effective approach to purify water, particularly to remove heavy metal ions, due to its high technical applicability, selective uptake and cost efficiency, especially for low-level heavy metal treatment in water [19]. The adsorption process works by mass transfer from the liquid phase to the solid phase, which is referred to as the adsorbent. The sorption of the contaminants onto an adsorbent consists of three main stages: (I) the diffusion of the contaminants in the solution to the surface of the adsorbent; (II) the adsorption of the contaminants on the adsorbent surface; and (III) contaminants diffusion on the structure of adsorbent [20]. In addition, the removal of metal ions by adsorption has the great advantage that the process can run in reversible mode and the adsorbents can be reused after regeneration using a suitable desorption process. Currently, the most commonly used adsorbents are synthetic polymers or inorganic materials, such as ion-exchange resins, activated carbon and zeolites, which have disadvantages such as high manufacturing costs and non-renewability and the potential for secondary damage of water bodies due to material leaching [21]. This is one of the reasons to develop more efficient, inexpensive and environmentally friendly absorbent materials for water treatment. The adsorption capabilities of a number of low-cost adsorbents, such as biomaterials, have been determined for the removal of heavy metals from water, demonstrating that cellulose and its derivative materials show good adsorption capacity towards heavy metal ions [15].

### 2.2.2. Use of biosorbents in the removal of heavy metal ions

Biomaterials are attracting increasing interest as efficient adsorbent and filter materials for water treatment, as they can be derived from various biomasses. Biopolymers, such as cellulose, are cost effective due to their high abundance and renewability [22]. Cellulose, one of the most abundant natural biopolymers, is an excellent raw material for the production of biosorbent materials [23]. Cellulose is a linear homo-polysaccharide composed of β-1,4-linked

anhydro-D-glucose units with the repeating unit cellobiose containing six hydroxyl groups, which form strong inter and intramolecular hydrogen bonds. The hydrogen bonding networks in the crystalline sections of cellulose are strong and densely packed, resulting in a durable, fibrous, highly resistant and water-insoluble cellulose fiber. In addition, a great number of available OH-groups allow cellulose to be modified into a material with greater functionality [24]. Cellulosic materials with specified nano-scale structural dimensions are referred to as nanocellulose, which is a natural nanomaterial that is non-toxic, biodegradable and biocompatible with no harmful effects on human health and the environment. There are three major types of nanocellulose: cellulose nanofibrils (CNF), cellulose nanocrystals (CNC) and bacterial nanocellulose (BNC) [25]. These nanocelluloses can be extracted from renewable and abundant resources, such as any cellulose containing biomass by using top-down approaches or bottom-up methods utilizing bacteria. CNF and CNC are usually obtained from plant sources, such as wood pulp, crop or agricultural waste streams, via the top-down approach, which include chemical, mechanical and/or enzymatic processes (Figure 2). BNC is generated using a bottom-up method that involves cellulose-producing bacteria fermenting low molecular weight sugar. For the isolation of CNC, chemical treatments such as acid hydrolysis is performed, by which the disordered/amorphous regions of the cellulose fibres are hydrolysed, while the crystalline sections are maintained [26].

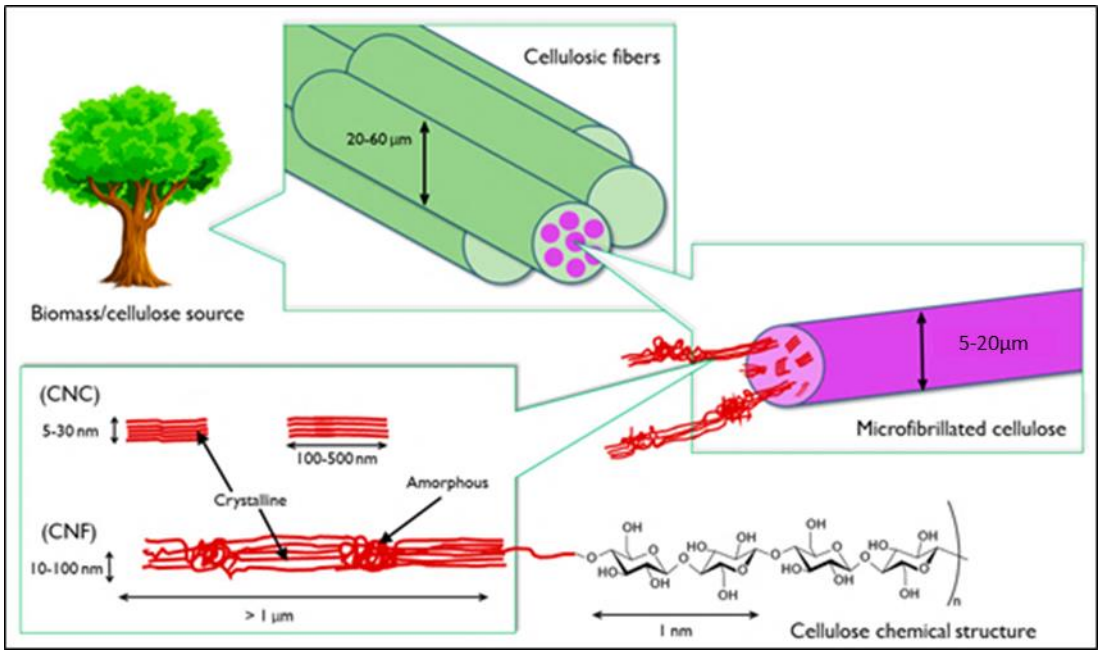


**Figure 2: Schematic representation of the extraction of CNF and CNC from cellulosic biomass [27].**

The specific surface area, crystallinity as well as number of surface hydroxyl groups increase tremendously when cellulose is converted into nanocellulose [15]. Nanocellulose can be tailored for selective and improved interactions through a variety of chemical modifications thanks to its high number of surface hydroxyl groups. Besides, these groups act as active sites for the fabrication of functional adsorbents with high capacity [28]. Nanocellulose is appealing for applications in a variety of fields, including nanocomposite materials, surface modified materials, papermaking, food packaging, coating additives and textiles. The surface modification processes of nanocellulose expand their potential applications as functional adsorbents in the environmental sector, including water purification and pollutants removal [29].

## 2.3. Nanocellulose in water treatment

The number of potential applications of sustainable and environmentally friendly products from natural resources has increased in various fields in recent years as they show enormous potential for reducing cost and increasing efficiency in pollution treatment and clean-up [22]. In particular, biodegradable and non-toxic materials including cellulose-based materials have received widespread attention [17]. Nanocellulose is commonly used as an excellent natural biomaterial adsorbent for environmental remediation technologies due to its natural abundance, non-toxicity, renewability, sustainability and the possibility of surface modification [30]. In addition, properties of nanocellulose, including high mechanical strength and rigidity, are favourable for high-pressure water treatment [31]. In nanocellulose-based adsorbents, surface functionalisation is an important step in order to promote pollutant adsorption and increasing adsorption capacity. Surface modified nanocellulose by different strategies can remove numerous water contaminants, such as dyes, oils and metal ions, from water [32]. Nanocellulose based filters have two principle mechanisms for the separation of pollutants: separation by retaining particles larger than their pore size and adsorption of charged contaminants via electrostatic interaction on the surface of the filter [2]. Nanofiltration membranes can remove basically all types of viruses as well as many inorganic and organic molecules including divalent ions due to a small pore size of less than 2 nm [33].

### 2.3.1. Surface modification of nanocellulose

The surface of nanocellulose can be easily modified through chemical modifications because of its large surface area and abundance of hydroxyl groups. Chemical modification improves certain properties of nanocellulose, such as selective adsorption capacity for contaminants, by enhancing the number of active bonding sites and creating new functional groups that support the absorption of certain classes of compounds [34]. Carboxylation, sulfonation, oxidation, phosphorylation, esterification, etherification and amidation are some of the techniques used to attach functional groups or molecules on the nanocellulose surface. Figure 3 illustrates several possible approaches for the chemical functionalisation of nanocellulose structures. Introduction of functional groups on the surface of nanocellulose allows to change its (surface) properties required for various applications [35].

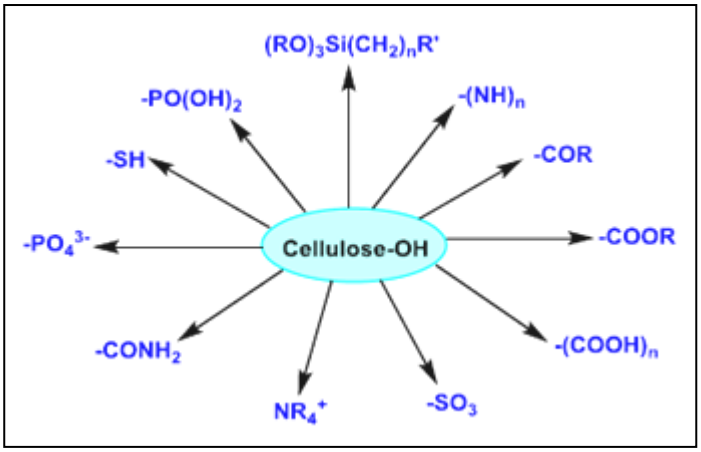


**Figure 3: Main routes of surface functionalisation of nanocellulose for the adsorption of pollutants [9].**

Among the these functionalisation methods, the introduction of carboxylate groups to CNF surfaces is one of the most studied methods as they exhibit high adsorption efficiency, stability and regeneration capability for the removal of hazardous pollutants in particular multivalent metal ions, including Cu(II) ions [36]. For the carboxylation of CNF, two general strategies have been developed: (1) direct chemical modification by oxidation or etherification. These methods usually involve complicated modification procedures and the use of hazardous organic solvents and (2) introducing carboxylate groups on the surface of CNF using 2,2,6,6-tetramethylpiperidin-1-oxyl (TEMPO). This approach is a promising method for the preparation of CNF with a high number of carboxyl groups due to its ability to transform hydroxyl into carboxyl groups. TEMPO-CNF exhibit a high number of negatively charged carboxylic ($COO^-$) functional groups, which are beneficial for the adsorption of positively charged heavy metal ions, for instance copper (II) ions [37].

### 2.3.2. TEMPO-oxidation of cellulose

TEMPO is widely used as oxidising agent for cellulose due to its reversible redox behaviour and high catalytic efficiency. In addition, TEMPO is a stable nitroxyl radical, which is water-soluble and commercially available [38]. The primary C6-OH groups of cellulose are selectively oxidised into carboxylic groups using catalytic oxidation with TEMPO without changes to the original crystallinity. Figure 4 shows the oxidation mechanism of cellulose by TEMPO. The C6-OH group ($CH_2OH$ of (1)) of cellulose is selectively converted into carboxylate groups (COOH of (3)) via an aldehyde intermediate (CHO of (2)), consuming NaClO and NaOH. Aldehyde groups in the oxidation products have an impact on the separation and stability of oxidised cellulose. Therefore, the TEMPO/NaCl/NaOH-oxidation system avoids the presence of aldehyde groups in the final product by immediately oxidising then into carboxylate groups by NaClO [39]. Furthermore, alkaline conditions promote the dissociation of the primary hydroxyl groups, resulting in a faster production of covalent bonds than at neutral or acidic conditions [40]. The reaction mixture is typically maintained at basic conditions (pH ≈ 10), which transform the carboxylic acid moiety into the carboxylic acid sodium salt moiety (COONa of (4)) [41].

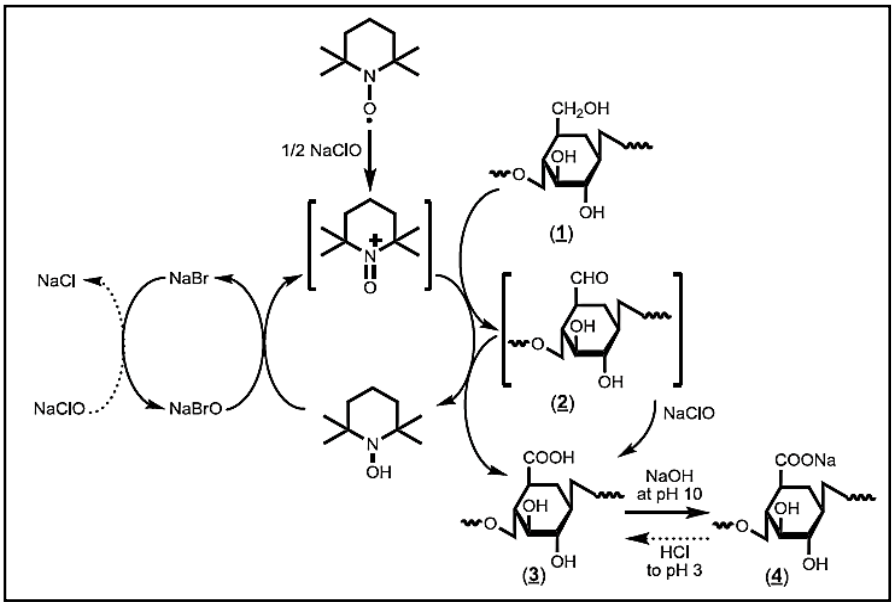


**Figure 4: Scheme of the selective oxidation of the primary C6-OH group of cellulose to carboxylate groups by TEMPO/NaClO/$NaClO_2$ oxidation in water at pH 10 - 11 [37].**

The oxidation process can be controlled by adding NaOH to the reaction mixture to keep the pH at 10 during the reaction. Furthermore, NaClO plays an important role in the oxidation process as the amount of carboxylate groups converted from the primary OH groups of cellulose can be controlled by varying the amount of NaClO added. TEMPO mediated

oxidation is highly efficient generating high amounts of anionic carboxylate groups, which are introduced as functional groups on the cellulose surfaces [42]. After TEMPO oxidation, low energy blending is sufficient in order to disintegrate cellulose fibers into nanocellulose. Due to the COOH groups and their repulsion, very low fibril diameters can be obtained at lower energy input. Films produced from TEMPO oxidised cellulose nanofibrils (TEMPO-CNF) exhibit high light transmittances, high mechanical strengths and very low oxygen permeabilities under dry conditions [40]. In addition, TEMPO-CNF could be of interest to applications for water purification because of its low energy consumption, high yield and uniform morphology [43].

### 2.3.3. Adsorption mechanism of heavy metal ions on TEMPO-CNF

Adsorption of metal ions on TEMPO-CNF is achieved by complexation or electrostatic attraction between CNF and metal ions. The carboxyl groups on the surface of TEMPO-CNF act as active sites for the removal of metal ions. Cu(II) ions diffuse to the surface of TEMPO-CNF during the removal process where they are electrostatically attracted (1) by the negatively charged carboxylate groups. Then, $Na^+$ and $H^+$ ions are replaced by Cu(II) ions by ion exchange (2), while Cu(II) ions are partly also captured by two carboxylate groups via complexation (3) (Figure 5) [43].

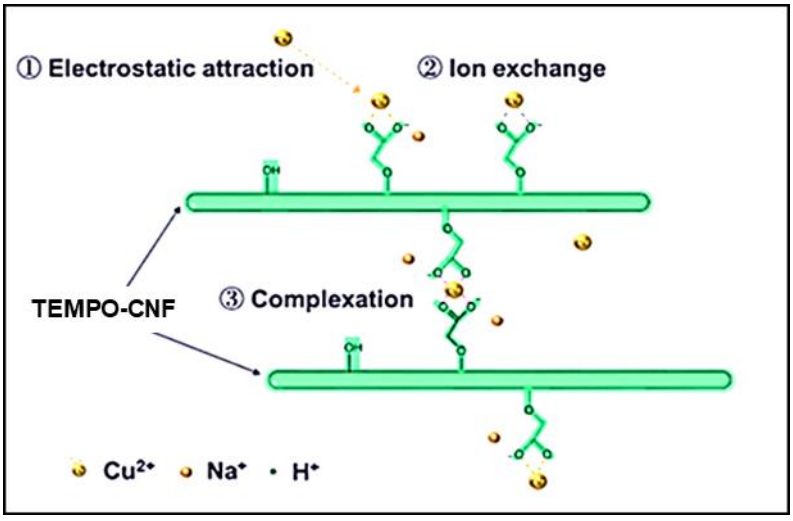


**Figure 5: Mechanistic model of Cu (II) adsorption by TEMPO-CNF filters. The light orange shadow refers to electric static interaction [43].**

The carboxylate content of TEMPO-CNF is an important factor that affects the adsorption of heavy metal ions, such as Cu(II) ions, using TEMPO-CNF filters [14]. Apart from heavy metal ions, TEMPO-CNF filters potentially also adsorb earth alkaline metal ions, e.g. calcium and magnesium, thus exhibiting high potential for the reduction of water hardness [44]. A significant

benefit of TEMPO-CNF filters is that they can be regenerated using appropriate chemical methods. This is a critical parameter to determine the applicability of these materials from an economic point of view. A variety of methods has been suggested and tested, depending on the adsorbed species, to regenerate nanocellulose-based filters. Frequently, filters saturated with heavy metal ions are treated using an acidic or alkaline solution [20], facilitating the desorption of metal ions from TEMPO-CNF filters such that the filter can be reused [45].

## 3. Aims and objectives

The aim of this work was to establish the utility of pilot-scale flat filters containing TEMPO-CNF as functional adsorption agent for the removal of heavy metal ions produced by coating and drying foamed (referred to as foam coating) and non-foamed (referred to as cast coating) TEMPO-CNF suspensions. In order to facilitate highly efficient filters with high permeance a coating method was needed that allows application of small amounts of nanocellulose in thin layers. To achieve this aim, the following objectives were defined with the coating process operated at pilot-scale. Two coating methods should be applied in order to control the coat weight, which was hypothesised to influence the heavy metal ions removal of the resultant filters. The performance of the filters should be characterised by water permeance and removal of Cu(II) ions, as model for heavy metal ions, by adsorption experiments. The influence of the pH on the heavy metal ions adsorption and the reusability of the filters are also to be investigated. Furthermore, the morphology and mechanical properties of the TEMPO-CNF coated filters should be assessed.

# 4. Experimental section

## 4.1. Materials and methods

TEMPO-CNF suspension (1.1 mmol/g of carboxyl groups) was produced and supplied by Swiss Federal Laboratories for Materials Science and Technology (EMPA). Hotstapur SAS 30 (Secondary alkane sulfonate $CH_3 – (CH_2)_m – CH\text{-}(SO_3Na) – (CH_2)_n – CH_3$) was purchased from Clariant. Viscose fabric was supplied by Acondaqua (Spain). All reagents were of analytical grade. $CuCl_2$ (97 %), ammonium chloride (97.5%), Murexide, HCl (37 %) and NaOH were purchased from Sigma-Aldrich. Ethylenediaminetetraacetic acid (EDTA) was purchased from W. Neuber's Enkel (Vienna, Austria). All chemicals were used as received without further purification and ultra-pure water (0.05 µS/cm, Elga Pure lab, High Wycombe, UK) was used for all procedures.

## 4.2. Preparation of foam and cast coated TEMPO-CNF filters

Foam and cast coated TEMPO-CNF filters were produced at VTT Technical Research Centre of Finland. Surface coating of the viscose fabric was carried out by two methods, foam and cast coating. All coatings were made on the Surface Treatment Concept (SUTCO) pilot coating machine located at VTT (Espoo, Finland). For foam coating, the TEMPO-CNF suspension with 1.7 wt % solid content (dry TEMPO-CNF) was mixed with 1.5 wt % SAS 30 as foaming agent. The mixing was done gently to avoid any air entrapping before foaming. The homogenous dispersion was then fed to a foam generator (Hansa Top-Mix, Hansa Industry Mixer GmbH). Compressed air was injected into the foam generator and the suspension frothed under shear created by a rotor-stator assembly. The airflow rate was automatically controlled by the flow rate of the liquid suspension and the predefined foam density. The produced foam was then pumped to the coating station of the pilot machine where it was applied on the moving web through a slot-die. The die had a width of 250 mm and the slot-web gap (SWG) was fixed at 1 mm. A schematic of the foam coating process is shown in Figure 6. After foam deposition, the web was run over a vacuum box (under pressure 4-5 kPa) to enhance the penetration of the foam into the bulk of the substrate. The coated wet web subsequently entered the drying section, which was composed of three separate infrared drying units (12-14 kW each) and five convection drying units (140 kW each). The water in the foam was evaporated, hence the foam collapsed and dry TEMPO-CNF was deposited on the substrate. The line speed was varied between 2.5 and 4 m/min for the foam coating process to control the coat weight.

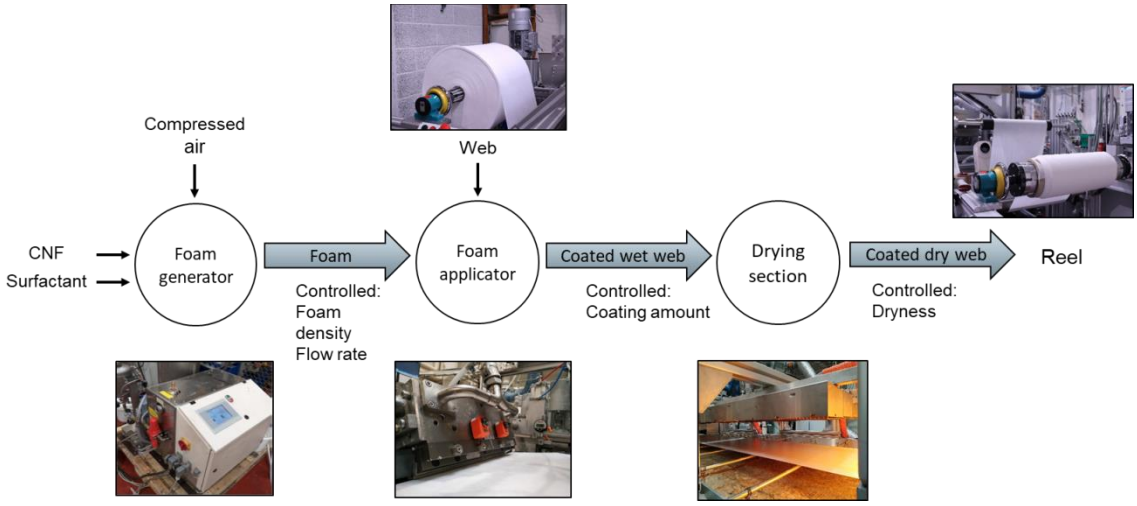


**Figure 6: Schematic of the roll-to-roll foam coating process on the SutCo pilot line [Source: VTT].**

Cast coating was used to apply higher coat weights of CNF on the substrate as compared to foam coating. The CNF suspension containing up to 1.7 % solid content was fed into the coating feed (Figure 7) and the bottom of the reservoir was opened towards the machine direction. The opening size, denoted as the casting gap, was measured as the vertical distance between the bottom surface of the casting bar and the web. The coat weight during casting depends on both the line speed and the casting gap. The coating width was kept constant at 300 mm and the line speed was fixed at 1 m/min. Hence, the theoretical coat weight depended only on the casting gap and the solids content of the CNF suspension. Cast coating was followed directly by drying the web, the vacuum box was not used as the high amount of coating was observed to cause penetration of the CNF suspension to the backside of the web and exiting it. The cast coated substrates were dried in batch method. Due to the high coat weight and thus high water content, the web was kept in the IR drying section for 30 min to evaporate all the water.

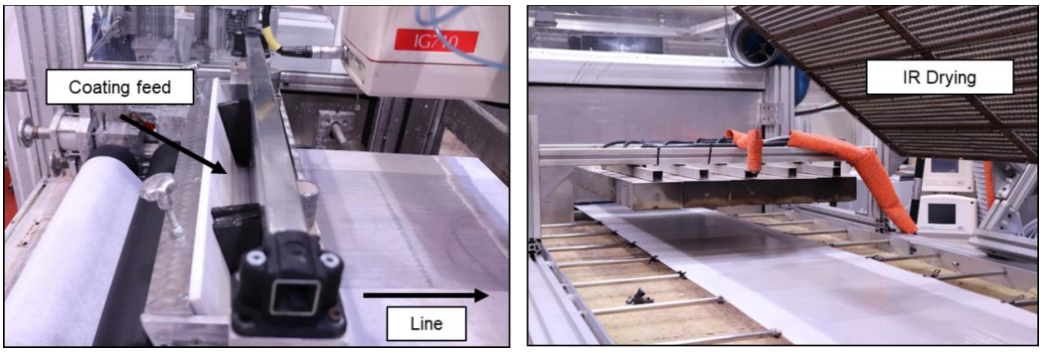


**Figure 7: Casting station (left) and drying section (right) of the SutCo pilot line.**

## 4.3. Characterisation of foam and cast coated TEMPO-CNF filters

### 4.3.1. Coat weight, shrinkage and thickness of filters

Discs with a diameter of 0.24 m were cut from the foam and cast coated TEMPO-CNF filters. The filters were weighed and the filter area was determined by ImageJ (Fiji). The grammage [G] of the filter was calculated with Equation 1.

$$\mathrm{G}\left[\frac{\mathrm{g}}{\mathrm{m}^2}\right] = \frac{\text{Mass of the filter [g]}}{\text{Area of the filter [m}^2\text{]}} \qquad (1)$$

The foam coated TEMPO-CNF filters shrunk during the drying process and the shrinkage was calculated with Equation 2.

$$\mathrm{S} = 1 - \frac{\text{Width of coating [m]}}{0.25\ \text{[m]}} \qquad (2)$$

The actual width of the foam coated portion of the filters was measured at five different spots with a ruler. The set width of the coated filters was 0.25 m. After calculating the shrinkage, the real coat weight ($G_{rcw}$) of foam coated TEMPO-CNF filters was calculated with Equation 3.

$$\mathrm{G_{rcw}}\left[\frac{\mathrm{g}}{\mathrm{m}^2}\right] = \frac{\text{Set coat weight}}{1 - \text{shrinkage}} \qquad (3)$$

The grammage of uncoated and cast coated TEMPO-CNF filters was also calculated with Equation 1. The real coat weight of cast coated filters was then calculated with Equation (4).

$$\text{Real coat weight}\left[\frac{\mathrm{g}}{\mathrm{m}^2}\right] = (\text{grammage of cast coated filter}) - (\text{grammage of uncoated filter}) \quad (4)$$

The thickness of each test specimen of foam and cast coated TEMPO-CNF was measured at 3 different spots using a digital micrometre (electronic outside micrometre 0-25 mm, accuracy 0.001 mm).

### 4.3.2. Morphology of filters by scanning electron microscopy

The morphology of uncoated as well as foam and cast coated TEMPO-CNF viscose filters was assessed by scanning electron microscopy (SEM, JCM-6000, JEOL, Germany). Prior to imaging, the samples were fixed onto SEM stubs using carbon tabs and gold coated for 1 min at 30 mA using a sputter coater (JEOL Fine coater JF-1200, Germany).

### 4.3.3. Pure water permeance of filters

The permeance of pure water through the filters was measured using a dead-end cell (Sterlitech HP4750 stirred Cell) at a backpressure of 0.2, 0.5 and 1 bar nitrogen at room temperature (21°C). Filters with a diameter of 49 mm were fixed on a porous stainless steel plate, which was then placed on top of the bottom part of the dead-end cell. Afterwards, the plate and cell bottom were clamped with the cell body. 200 mL of deionised water were filled into the cell body, which was sealed by the cell lid connected to $N_2$. At the desired backpressure deionised water was forced through the filter. The permeate water was collected in a measuring cylinder and the permeance time measured for each 50 mL of permeate. The permeance P was calculated using Equation 5:

$$P\left[\frac{L}{m^2 \cdot h \cdot MPa}\right] = \frac{V}{A \cdot t \cdot p} \qquad (5)$$

V is the volume of the permeate solutions collected, t is the time permeate was collected, A is the effective filtration area of the filter (1460 $mm^2$) and p is the backpressure forcing water through the filter. This permeance test was repeated three times for each of the three different pressures for each sample (Figure 8).

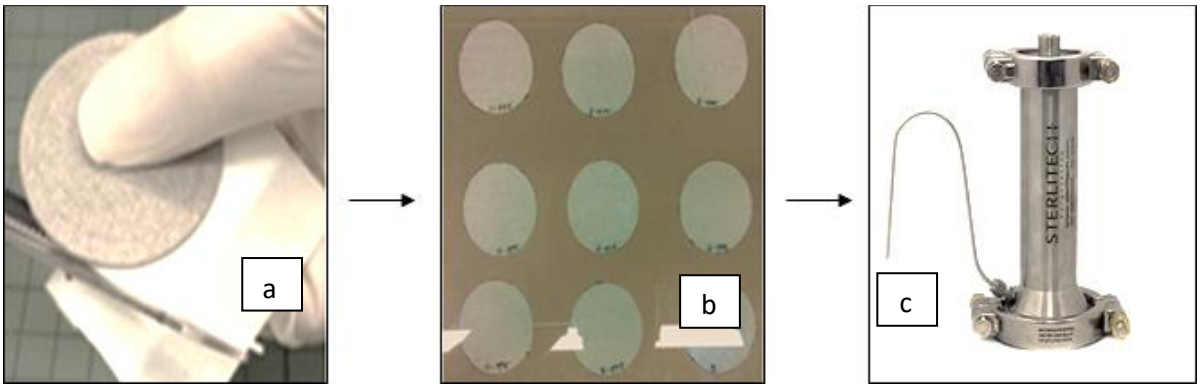


**Figure 8: a. Cutting of discs from filters, b. filter discs with a diameter of 49 mm for the pure water permeance and c. Sterlitech HP4750 dead-end cell.**

### 4.3.4. Adsorption of metal ions on filters

Two discs of the filters with a diameter of 0.24 m were placed in a Büchner-Funnel (Figure 9a and b). The funnel was fixed on a filter flask, which was connected to a water-jet pump. 200 mL test solution containing 2.5 mM $CuCl_2$ were filtered through the TEMPO-CNF coated filter under reduced pressure (Fig 9b) and the filtered solution was collected. Fresh test solutions

were filtered through the filters multiple times (usually 5 times) to reach saturation of the filters, i.e. the Cu concentration in the feed and filter solutions were identical within error. The concentrations of the feed and filtrate solutions were determined by titration. 50 mL of the permeate were pipetted into a 250 mL Erlenmeyer flask and mixed with 50 mL pure water. The pH was set to 10 by adding 5 mg of $NH_4Cl$ and 2 mL of 30% $NH_3$. Murexide was dissolved in the solution as colour indicator. A yellowish/greenish solution was obtained and titrated with 0.11 M EDTA until the transition point (colour change from yellow/orange to pink Figure 9c). The final concentration of Cu(II) ions in the filtered solution was calculated by Equation 6.

$$C_{(Cu^{2+})}\left[\frac{\text{mmol}}{\text{L}}\right] = \frac{0.11\,[\text{mol}\cdot\text{L}^{-1}]\cdot V_{\text{EDTA}}\,[\text{mL}]}{V_{\text{Titration}}[\text{mL}]\cdot 1000} \qquad (6)$$

$V_{EDTA}$ [mL] is the volume of EDTA, which was used to titrate the permeate solution. $V_{Titration}$ [mL] is the volume of solution that was titrated (50 mL). To calculate the amount of Cu(II) adsorbed from a certain filtration fraction, Equation 7 was used.

$$m_{Cu}\,[\text{mg}] = \left(c_{\text{feed}} - c_{\text{permeate}}\right)[\text{mmol}\cdot\text{L}^{-1}]\cdot 63.456\,[\text{mg}\cdot\text{mmol}^{-1}]\cdot V_{\text{permeate}}\,[\text{L}] \qquad (7)$$

$C_{feed}$ is the concentration of the feed solution and $c_{permeate}$ is the concentration of the permeate solution. 63.546 mg/mmol is the atomic weight of copper. $V_{permeate}$ is the volume of solution that was filtered through TEMPO-CNF membrane filters. The mass of adsorbed copper ions [mg] per unit filter area [$m^2$], the areic adsorption capacity $q_A$, was derived by Equation 8.

$$q_A\left[\frac{\text{mg}}{\text{m}^2}\right] = \frac{\text{mass of the adsorbed copper ions}\;[\text{mg}]}{\text{area of the filter}\;[\text{m}^2]} \qquad (8)$$

The adsorption capacity $q_e$ [mg/g], the mass of adsorbed copper ions [mg] per total mass of active adsorption agent [g], was then calculated by dividing $q_A$ [mg/$m^2$] by the coat weight [g/$m^2$] (Equation 9).

$$q_e\left[\frac{\text{mg}}{\text{g}}\right] = \frac{q_A\,[\text{mg}\cdot\text{m}^{-2}]}{\text{coat weight}\;[\text{g}\cdot\text{m}^{-2}]} \qquad (9)$$

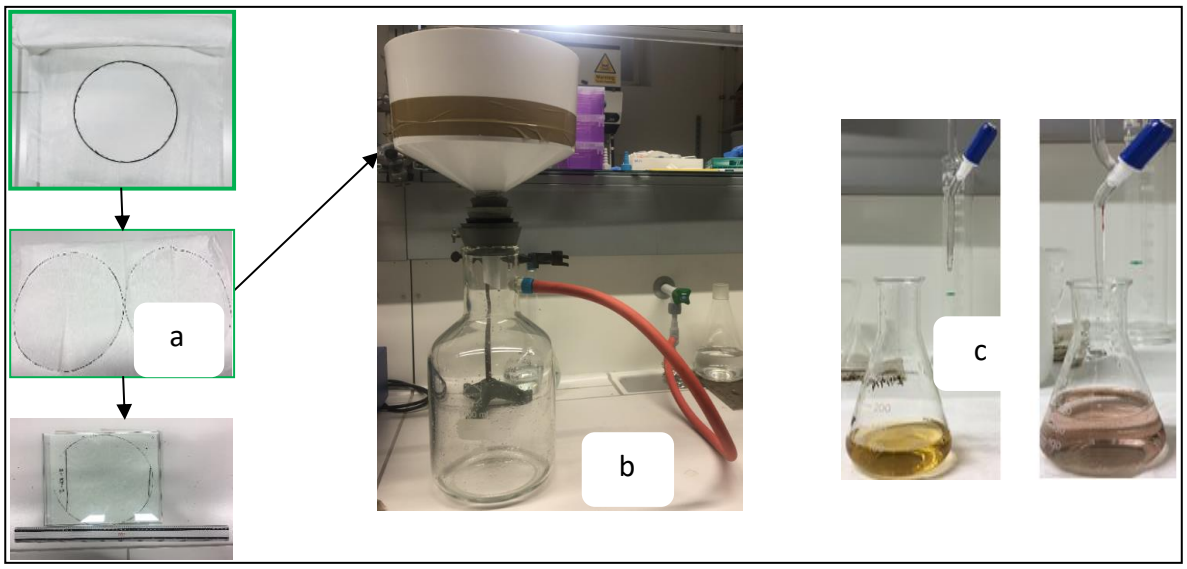


**Figure 9: a. Cutting of TEMPO-CNF filters, b. Büchner-Funnel and c. filtered copper chloride solution before and after the titration.**

To evaluate the influence of the pH value of aqueous solution on the adsorption capacity of heavy metal ions the filters were soaked in aqueous solution containing NaOH (pH = 10) or HCl (pH = 3), respectively, for 3 h. After soaking the filters were washed with deionised water to pH = 7 and dried at room temperature. Afterwards, the areic adsorption [mg/m$^2$] of $CuCl_2$ of the filters was assessed using the method described above.

To determine Ca(II) ions absorption onto the foam coated TEMPO-CNF filters, an adsorption study was performed with an aqueous solution of 2.5 mM $CaCl_2$. The experiment was carried out using the same method as for Cu(II) described above and the adsorption was calculated using the same equations but with the atomic weight of Ca (40.08 g/mol).

### 4.3.5. Regeneration of filters

After the adsorption test, two discs of the filters with a diameter of 0.24 m with adsorbed Cu(II) were soaked in 200 mL of 0.01 M HCl for 2 h. During this process, the pH value of the soaking solution was checked with pH indicator paper every 30 min. The acidic solution was then collected in a measuring cylinder. The concentration of Cu(II) ions was analysed by titration as described above and the mass of Cu(II) removed from the filter was determined. The regenerated TEMPO-CNF filter was rinsed several times with deionised water to pH = 7 and dried at room temperature. Afterwards, adsorption tests were conducted as described above to evaluate the regenerated TEMPO-CNF filters.

### 4.3.6. Leaching of surfactant or substrate from coated filters

Six pieces of 20×20 mm filters were cut from the coated TEMPO-CNF filters and samples 3, 6, 11 and 13 (Tables 1 and 2) were selected for this experiment for their high coat weight. Each three of those pieces were put into the tubes containing 10 mL deionised water or 0.01 M HCl, respectively. The tubes containing the pieces and leaching solutions were hand-shaken for 1 min then the pieces of filters were soaked therein for three h at room temperature (Figure 10 a and b). The soaked pieces of the filters were taken out from the solutions and visually inspected.

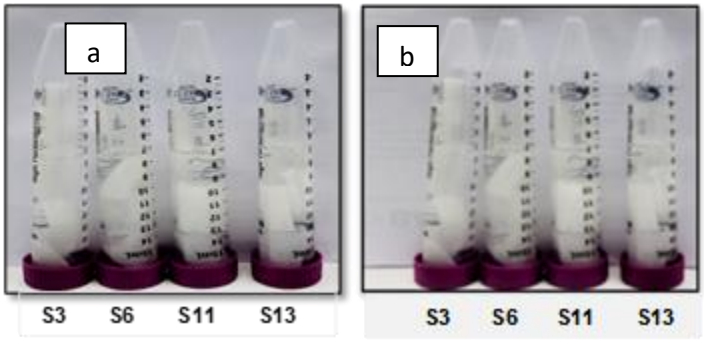


**Figure 10: Pieces of filters soaking in 10mL a. $H_2O$ and b. HCl.**

### 4.3.7. Mechanical properties of filters

Tensile tests were performed using a universal test frame (Model 5969 Dual Column Universal Testing System, Instron, Darmstadt, Germany) equipped with a 1 kN load cell. Dogbone shaped specimens with shapes according to ISO 527 type 5 were cut from each filter; the fiber direction of the filters was longitudinal to the specimens. The thickness of each test specimen was measured at 3 different spots using a digital calliper. To determine the mechanical properties of wet filters, specimens were soaked for 30 min in deionised water prior to the tests. Black dots were marked on the white coloured specimens along the longitudinal direction. The dry and wet specimens were clamped between two clamps with a distance of 25 mm. The specimens were stretched at a speed of 1 mm/min. The force during the tensile tests was recorded by the machine. A video extensometer (Blackfly-GigE-PoE) was installed around 1.5 m in front of the sample to evaluate the strain of the specimens. The gauge length was set to 20 mm and the deformation of the specimens during the tests was recorded from the dotted marks. Stress was calculated as the force per area ($N/m^2$ = Pa) and plotted as function of the strain. From the stress-strain curves, the mechanical properties, such as the ultimate tensile strength and the elongation at break, of the filters were obtained. The Young's modulus was calculated as the slope of the linear section of the stress-strain curves.

# 5. Results and discussion

## 5.1. Foam coated TEMPO-CNF filters

Foam coated TEMPO-CNF filters were designed for the removal of heavy metal ions from water. TEMPO-CNF was the active adsorbent on the viscose filter surface due to the presence of COOH groups, which facilitate capture of various heavy metal ions, such as Cu(II), from water. In order to maintain a high flux and a reasonable adsorption capacity, the amount of TEMPO-CNF coating needed to be controlled. Furthermore, TEMPO-CNF is quite expensive, hence, the first approach was filters with low coat weight. Ideally, viscose was coated in a way that individual viscose fibers are coated with a thin layer of TEMPO-CNF. However, using a TEMPO-CNF suspension directly as the starting material would lead to a prolonged drying procedure after coating of TEMPO-CNF considering the difficulty to remove water from the TEMPO-CNF network. Thus, a foamed TEMPO-CNF suspension was used as starting material for the coating. The foamed TEMPO-CNF was used to facilitate even coating layers desired at low coat weight.

The TEMPO-CNF suspension was foamed by mechanical whipping the suspension and injecting air in a rotor-stator mixer. The foam was stabilised by an anionic surfactant. The dry coat weight of TEMPO-CNF on viscose filters was set between 1.2 and 5.1 g/m$^2$. During foam coating and the subsequent drying process, the viscose filters were under tension in machine direction, retaining the dimension of the filters. However, in the transverse direction the filters were not under tension resulting in shrinkage upon drying. The extent of shrinkage was calculated using equation (2), reflecting the real coat weight. The real coat weight was between 1.3 and 6.8 g/m$^2$ (Table 1). For most samples, the shrinkage was about 20 %, with the shrinkage increasing with the set coat weight. Higher coat weight is connected to higher water content during drying and evaporating high amounts of water causing high stress in the transverse fiber direction, thus resulting in significant shrinkage. For all coat weights, but in particular for low coat weights, a reasonable agreement between set and real coat weight was found.

**Table 1: Set and real coat weights as well as shrinkage of foam coated filters.**

| Foam coated filters | Set coat weight [g/m$^2$] | Shrinkage | real coat weight [g/m$^2$] |
|---|---|---|---|
| Substrate | 0.0 | - | 0.0 |
| Sample 1 | 1.2 | 0.14 | 1.3 |
| Sample 2 | 1.2 | 0.20 | 1.4 |
| Sample 3 | 1.5 | 0.18 | 1.8 |
| Sample 4 | 2.5 | 0.0 | 2.5 |
| Sample 5 | 5.0 | 0.22 | 6.4 |
| Sample 6 | 5.1 | 0.25 | 6.8 |

In Figure 11 the thickness of foam TEMPO-CNF coated filters is plotted vs. their real coat weight. A linear relationship between the coat weight and the thickness of filters was observed, as anticipated.

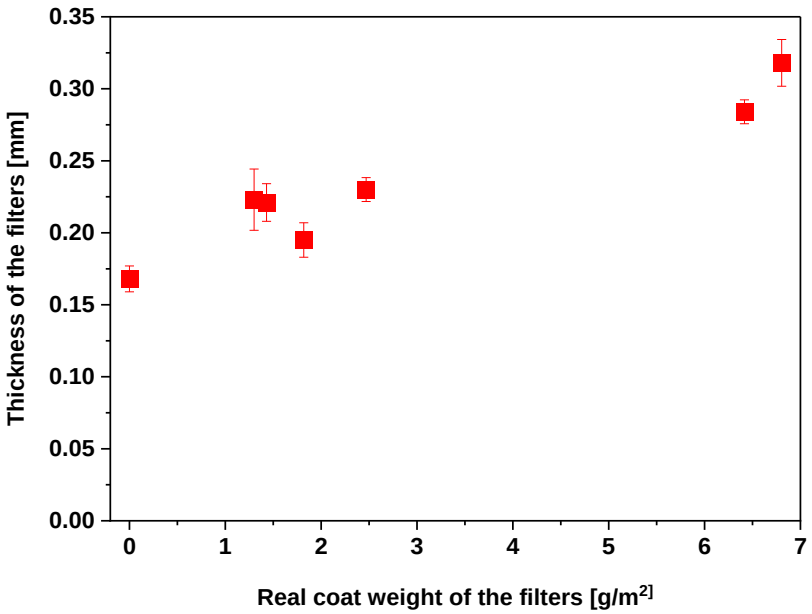


**Figure 11: Relationship between thickness and coat weight of foam coated filters.**

### 5.1.1. Morphology of foam coated filters

The surface and fiber morphologies of uncoated substrates and foam coated filters with different coat weights are displayed in Figure 12. Uncoated substrates consisted of non-woven fibers with a fiber diameter of 10-19 µm. Samples 1-5 with low and moderate coat weights had a similar surface morphology as the uncoated substrate. This was explained by the coat weights being too low in order to yield a dense surface layer of TEMPO-CNF. Sample 6 exhibited a dense but not continuous layer, caused by the highest coat weight of 6.8 g/m$^2$ as compared to samples 1-5. Nevertheless, the dense coating layer did not fully cover the top surface of the viscose substrate, leaving several holes. Furthermore, the bottom surface of Sample 6 showed loosely packed viscose fibers identical to other foam coated filters, indicating that the foam did penetrate through the filter to some extent.

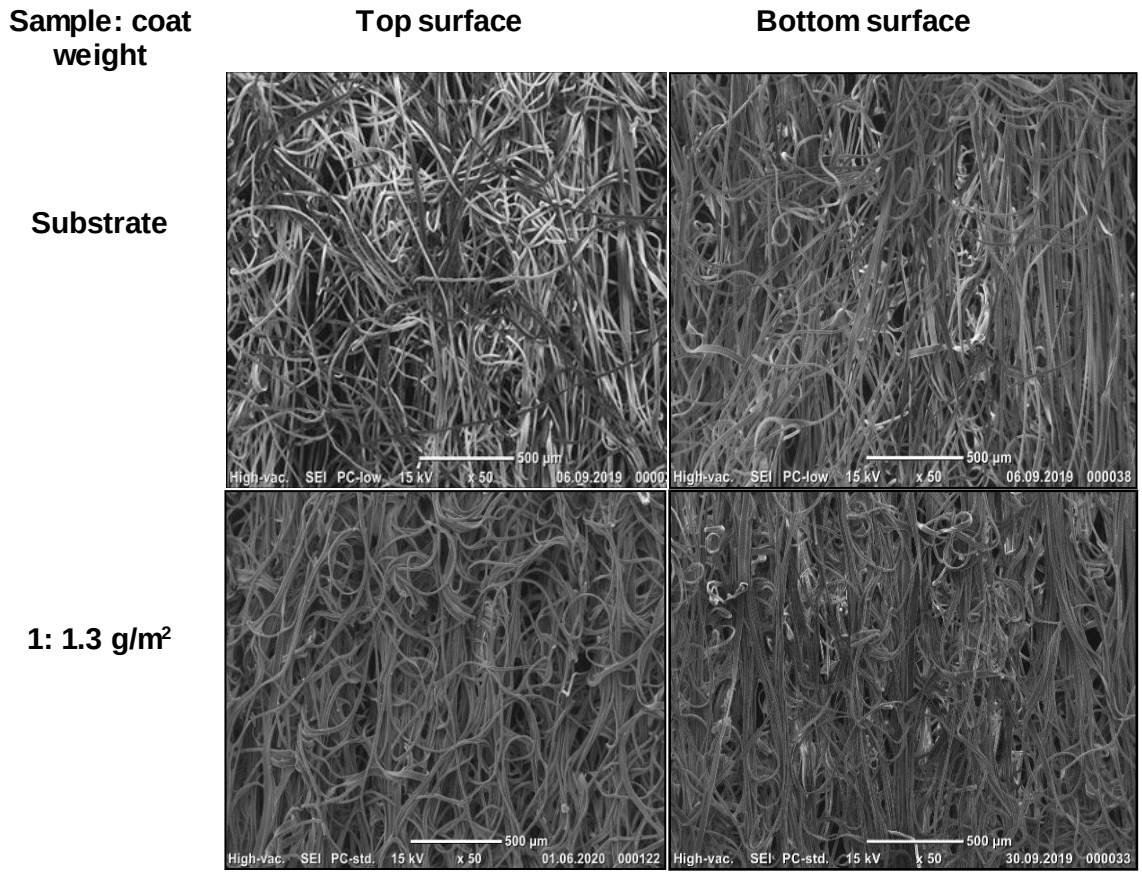

**2: 1.4 g/m²**

**3: 1.8 g/m²**

**4: 2.5 g/m²**

**5: 6.4 g/m²**

**6: 6.8 g/m²**

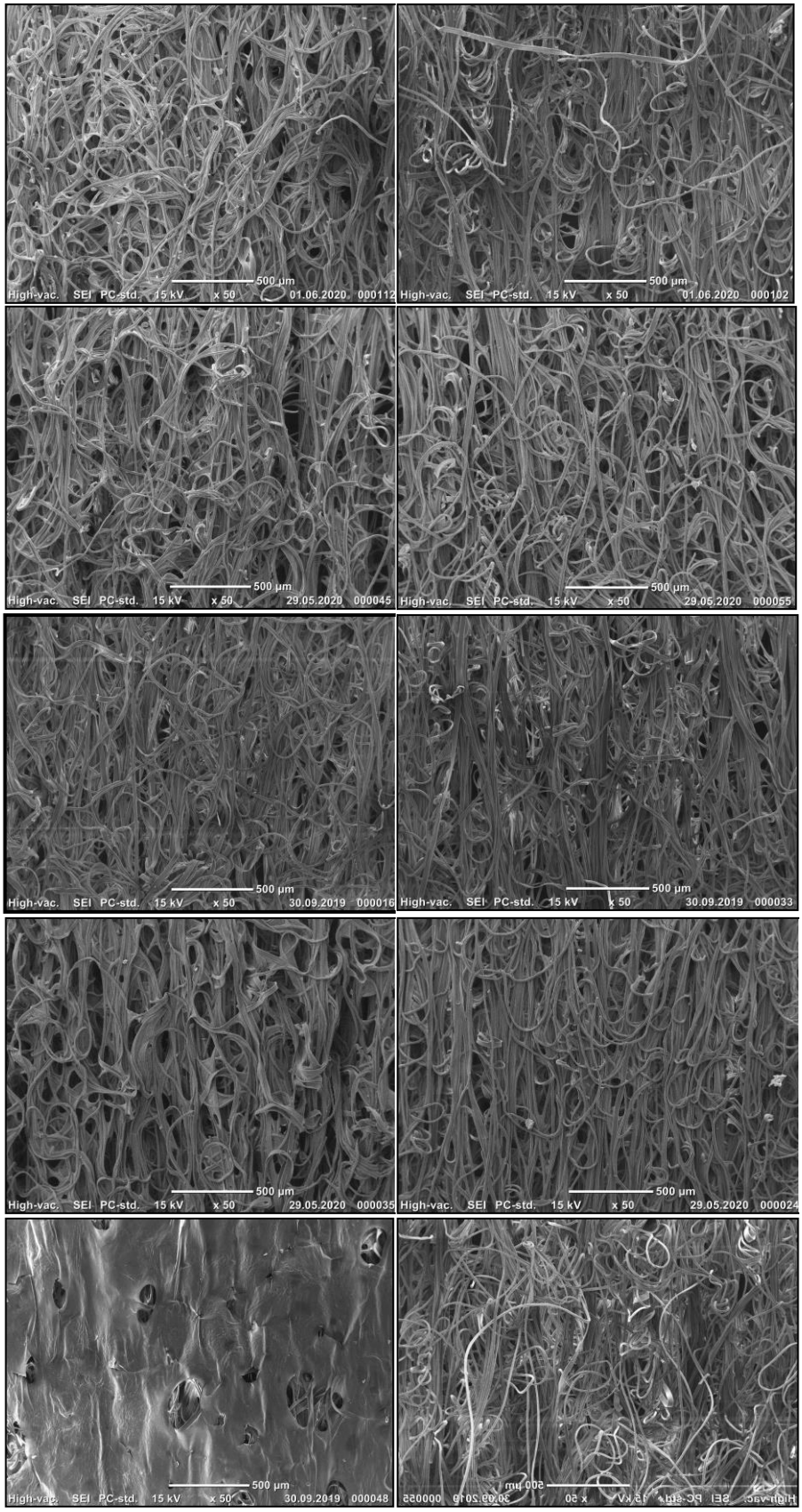


**Figure 12: SEM images of foam coated filters.**

TEMPO-CNF was present as a very thin film between fibers or coated on individual fibers (red arrows), respectively, as shown in Figure 13 displaying the surface of sample 1.

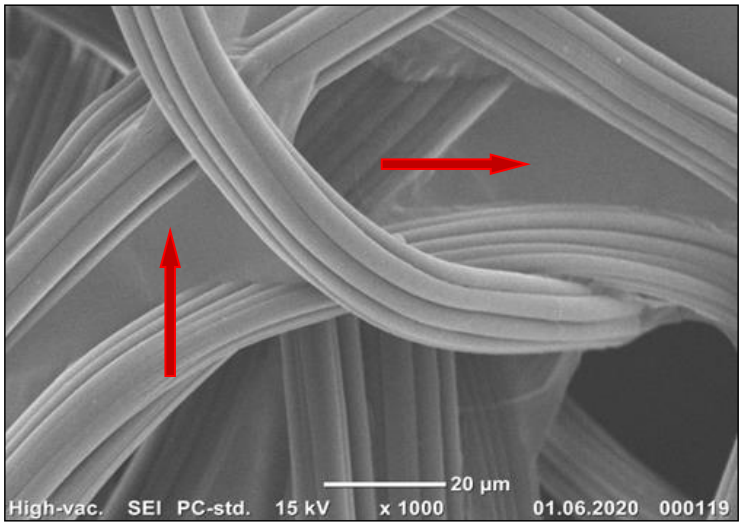


**Figure 13: SEM image of the surface of foam coated TEMPO-CNF filter/sample 1 at 1000× magnification. Red arrows indicate the presence of TEMPO-CNF.**

### 5.1.2. Pure water permeance of filters

The water permeance of uncoated and foam coated filters was measured using a dead-end cell at different pressures. Both uncoated and foam coated filters had similar water permeance ranging from 330000 to 430000 L / $m^2$ h MPa at 0.2 bar, indicating very fast water passage (Figure 14).

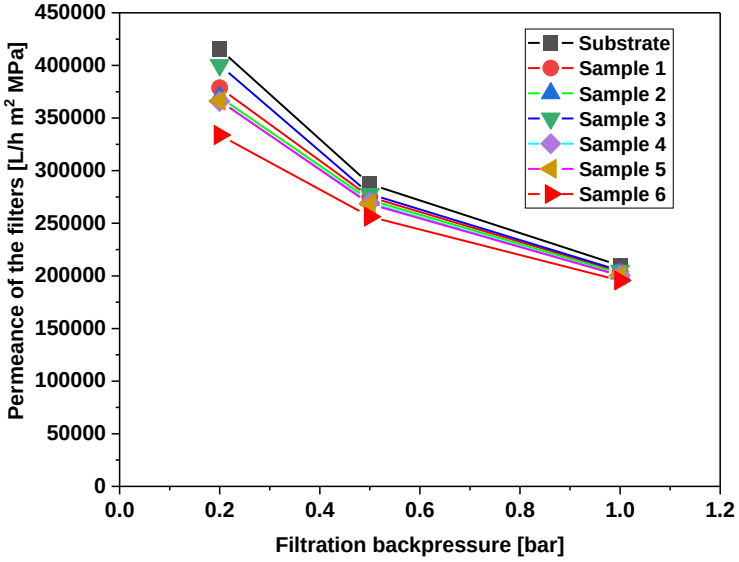


**Figure 14: Water permeance at different pressures**

Furthermore, the permeance slightly decreased with increasing coat weight (Figure 15). The high water flux was possible because of the high porosity and pore size of the viscose substrate hardly resisting water passage that was only slightly increased by the NC coating as no dense layer coating was formed, which functions as a barrier to hinder water to pass. For sample 6, which indeed had a dense but not continuous NC layer the permeance was lowest. Furthermore, the water permeance was reduced with increased pressure. This was explained by the compaction of the filters at higher pressure, resulting in a denser filter, whose water permeance was reduced. All filters thus permitted for high flux required in water filtration application.

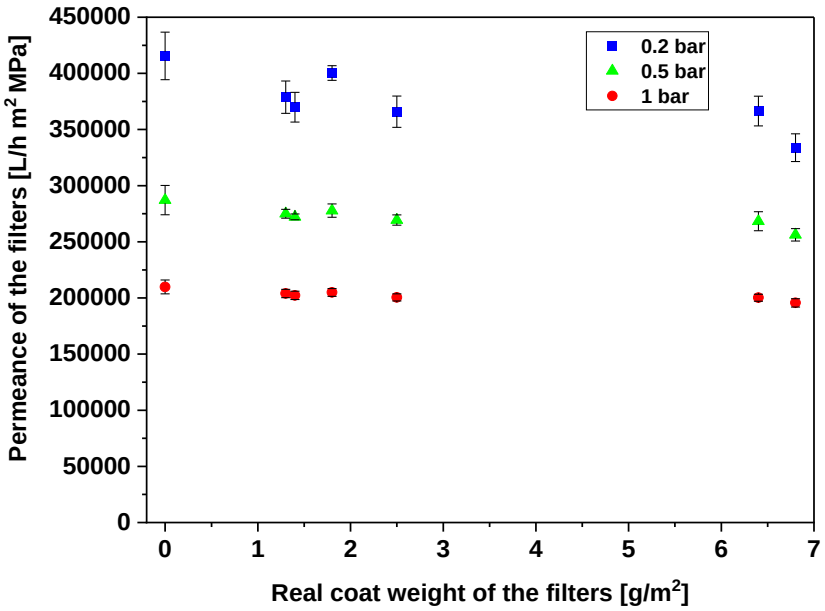


**Figure 15: Relationship between water permeance and coat weight of foam coated filters.**

### 5.1.3. Adsorption capacity for Cu(II) ions

2.5 mM $CuCl_2$ solutions, equivalent to 159 mg/L of Cu(II), corresponding to strongly copper contaminated water, was used as feed solution to investigate the adsorption capacity of the foam coated filters. The filtered solution was collected and the Cu(II) concentrations in the feed and filtered solutions were determined. The adsorption process of foam coated filters is summarised in Figure 16, which shows the volume-dependent adsorption of Cu(II) ions for all foam coated filters. It was determined that within 1000 mL (5 cycles of filtering), the filters reached saturation, i.e. the feed and filtered solutions had the same Cu(II) concentration.

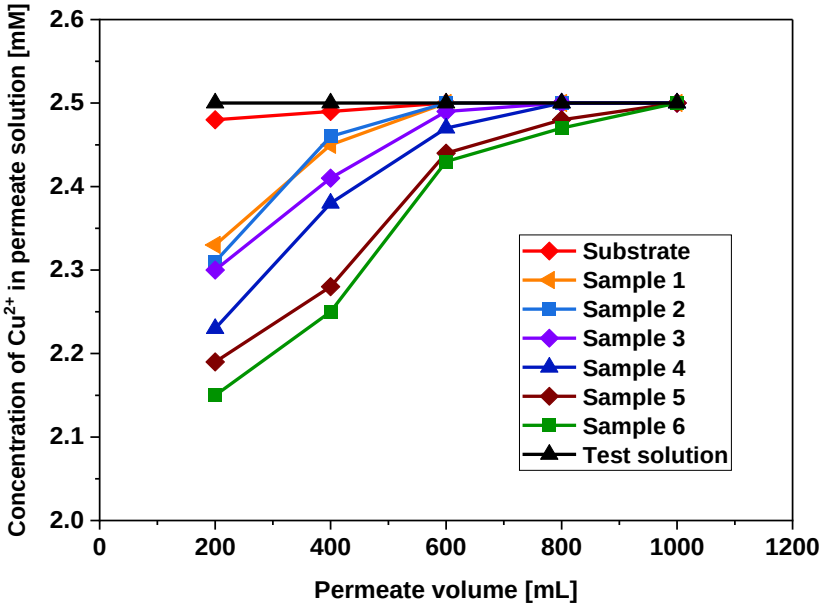


**Figure 16: Cu(II) adsorption of foam coated TEMPO-CNF filters.**

After the filtration, the foam coated TEMPO-CNF filters were coloured blue, indicating the adsorption of Cu(II) ions onto the filter surface. The adsorption of the foam coated TEMPO-CNF filters per unit filtration area are shown in Figure 17. The adsorption per unit area represents the areic adsorption of the filters when being used to adsorb heavy metals. With increasing coat weights to 6.8 g/cm$^2$, the adsorption per unit area increased from 25 to 128 mg/m$^2$. This was explained by the higher number of the carboxyl groups ($COO^-$) attached to the filter. The available $COO^-$ groups allowed for the adsorption of Cu(II) ions [44, 45].

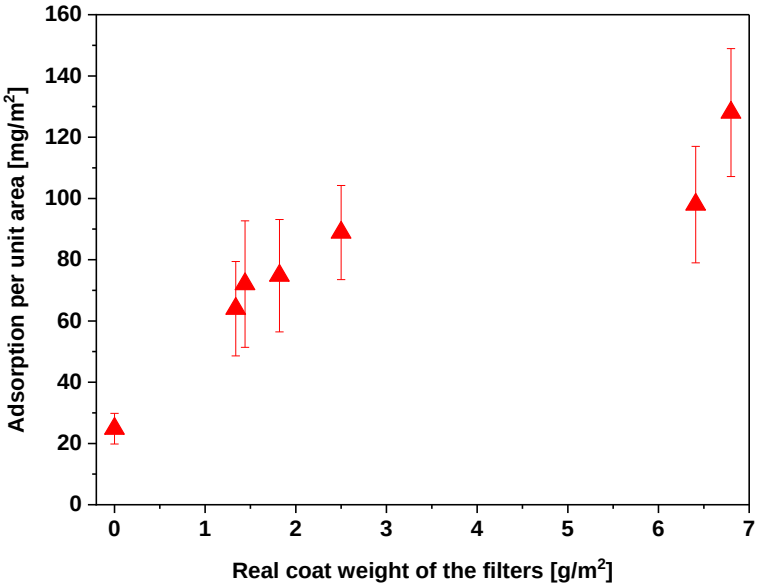


**Figure 17: Adsorption of copper ions [mg] per unit filter area [m$^2$].**

The adsorption capacity for various coat weights is shown in Figure 18. The adsorption capacity represents the adsorption per mass of TEMPO-CNF coating, allowing for consideration of cost efficiency. The adsorption capacity increased from 19 to 52 mg/g with decreasing coat weight, indicating that the adsorption efficiency was improved at lower coat weight. This was explained by establishing thicker TEMPO-CNF coating layers with increasing coat weight; considering that adsorption primarily occurs at the surface of TEMPO-CNF, increasing the coat weight, i.e. coating layer thickness, does not provide a higher number of $COO^-$ sites on or near the surface but rather buries them in the bulk of the coating. Thus, the adsorption capacity and coat weight were indirectly proportional. Comparison with the literature indicates that TEMPO-CNF showed an adsorption for Cu(II) of 75 mg/g [46] up to 135 mg/g [47], in the case of static adsorption on individualised fibers. Thus, adsorption capacities close to the one of individualised fibrils in static adsorption experiments were achieved but with the advantage of a continuous process.

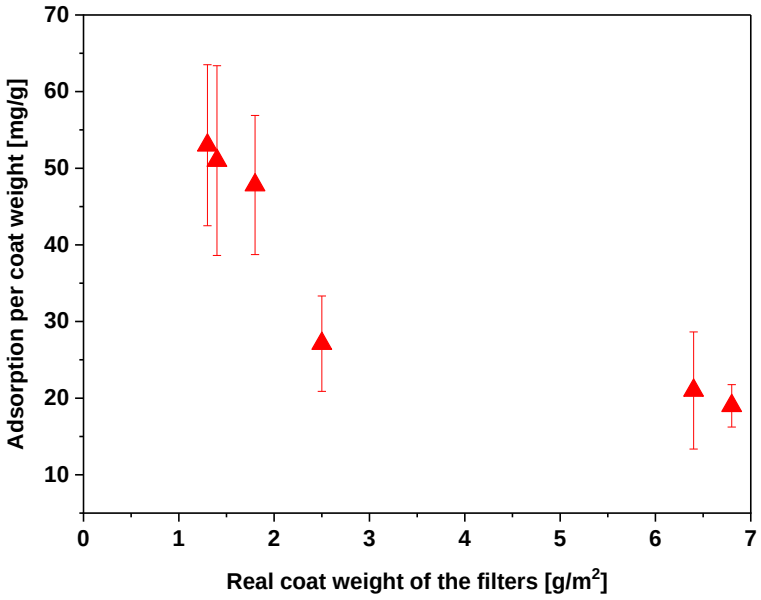


**Figure 18: Adsorption capacity, the amount of copper [mg] per mass active adsorption agent [g] as function of the real coat weight.**

It was anticipated that the pH of the aqueous these solution has a significant impact on the adsorption of heavy metal ions [44], because varying the pH value can change the state of functional groups on the surface of TEMPO-CNF and of metal ions in aqueous solution. Thus, in order to evaluate the influence of pH value on the adsorption of heavy metal ions from aqueous solution, the filters were soaked in alkaline (NaOH, pH = 10) or acidic solution (HCl, pH = 3), respectively. The areic adsorption for copper ions was then measured as in their

native state, showing that it was strongly reduced after soaking in alkaline or acidic solution (Figure 19). After soaking with NaOH and HCl, respectively, the adsorption capacity decreased from 75 mg/m$^2$ to 28.3 mg/m$^2$ and 31.6 mg/m$^2$ as well as from 128 mg/m$^2$ to 97.4 mg/m$^2$ and to 71.1 mg/m$^2$ for samples 3 and 6, respectively. The reduction of the areic adsorption under alkaline and acidic condition, respectively, might be explained by the protonation and deprotonation process of the carboxyl groups on the surface of filters and replacement of $H^+$ with $Na^+$, respectively. The carboxyl groups are protonated by an acid and deprotonated by a strong base [13]. In other words, the large numbers of charged $H^+$ or $Na^+$ ions, respectively, can reduce the attraction of surface $COO^-$ groups of the foam coated TEMPO-CNF towards adsorption of metal ions. In addition, those ions, in particular $Na^+$, are competing with Cu(II) ions to adsorb on the surface of the filter, thus reducing the interaction of the absorbent with the heavy metal ions [1].

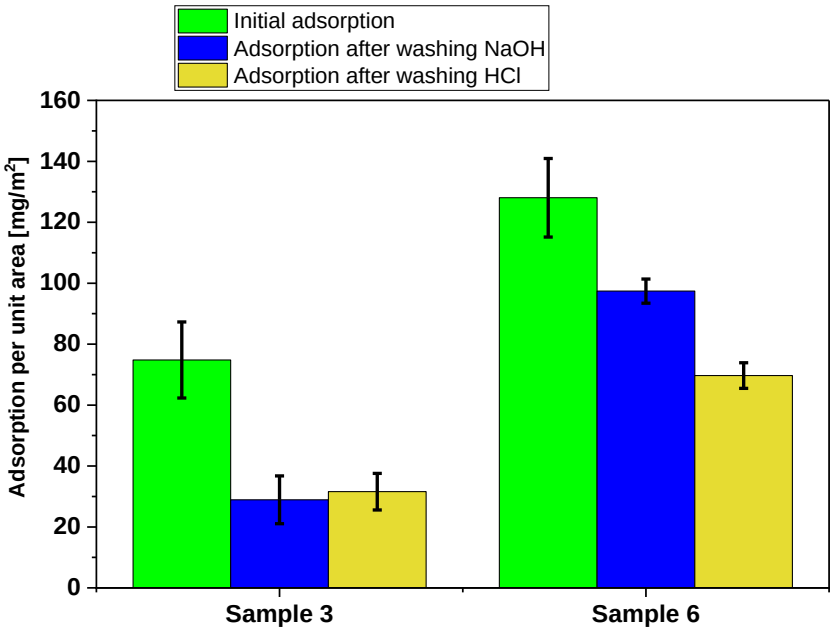


**Figure 19: Effect of pH on the adsorption.**

### 5.1.4. Regeneration and reuse of foam coated filters

Recyclability of filters is an important feature in practical applications and can benefit the economical value and the environment [48], as the active material of the filters is expensive and the amount of waste is reduced. After adsorption of Cu(II) ions filters were washed in HCl solution, which was proven before to be an efficient method to clean filters saturated with Cu(II) ions [49]. The washing process was optimal when soaking the filters in HCl at pH = 2 for 2 h. Figure 20 shows the amount of recovered Cu(II) ions from filters: 97 % of Cu(II) was recovered

from the filters. After a second washing procedure, the quantity of Cu(II) ions desorbed was basically zero, indicating that copper ions were majorly desorbed from the foam coated TEMPO-CNF filters already after the first washing step.

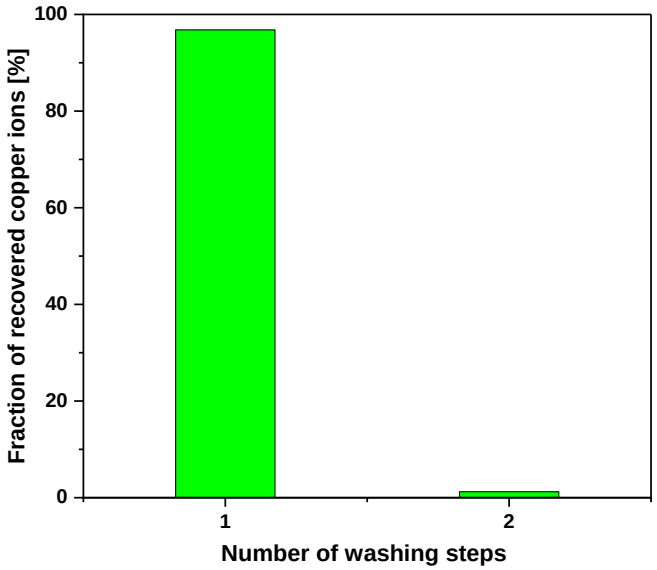


**Figure 20: Recovery of Cu(II) ions from foam coated TEMPO-CNF filters (Sample 6).**

After desorption of Cu(II) ions, TEMPO-CNF coated filters were subjected to a second filtration test. Re-adsorption capacities of 94 mg/m$^2$ and 54 mg/m$^2$, corresponding to 73 and 72 % of the original adsorption capacity for samples 6 and 3 regenerated filters, respectively, were observed (Figure 21).

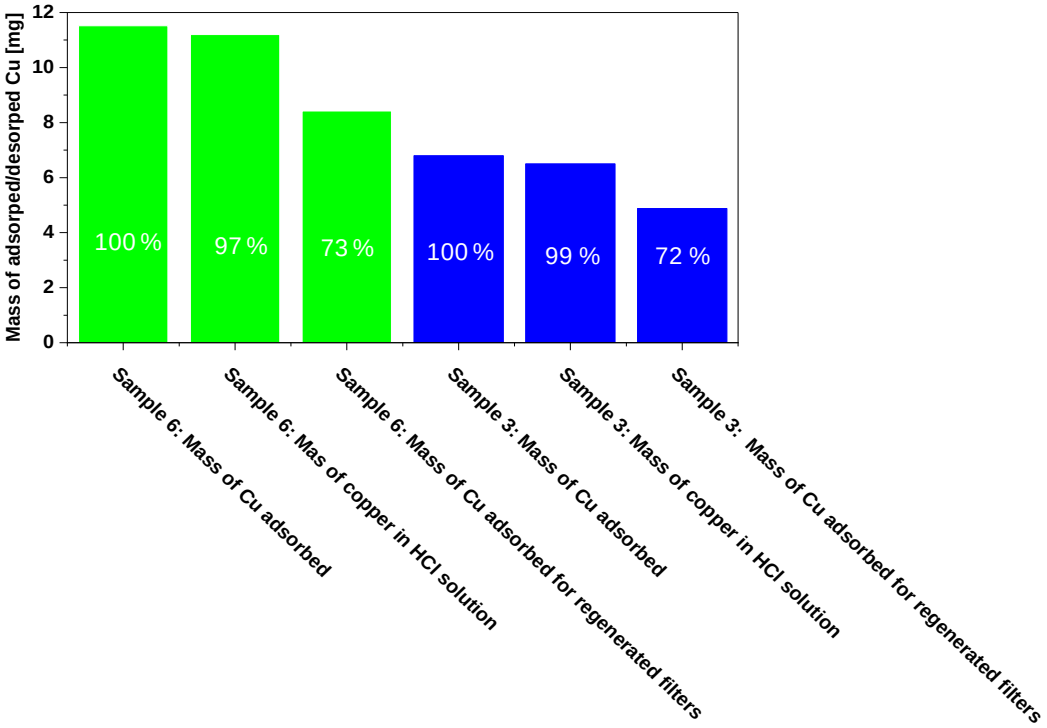


**Figure 21: Desorption and adsorption performance of (regenerated) foam coated TEMPO-CNF filters.**

### 5.1.5. Leaching of surfactant from foam coated filters

Leaching of matter into a water resource from the filters during practical application is required to be avoided to prevent secondary contamination. Leaching experiments were carried out to investigate whether the surfactants used for foaming of TEMPO-CNF leach from the filter. After soaking and shaking filters in HCl and water, respectively, liquid foam was observed to be present on top of the washing solutions, in particular for filter sample 6 with the highest coat weight (Figure 22). This indicated leaching of the surfactant, which acted as a foaming agent. Higher amounts of liquid foam were found for sample 6 compared to sample 3, which means a higher amount of surfactant having been present in the filter capable of leaching. Furthermore, fiber fragments of the viscose substrates were found in the liquid phase, which was because of the loose fiber network from which some fibers had escaped the filters during shaking. Thus, for application in real filtration applications, appropriate removal of surfactant would have to be carried out and the filter substrate consolidated, e.g. by sufficient amounts of CNF to bind the non-woven fibres, for instance by double-sided coating.

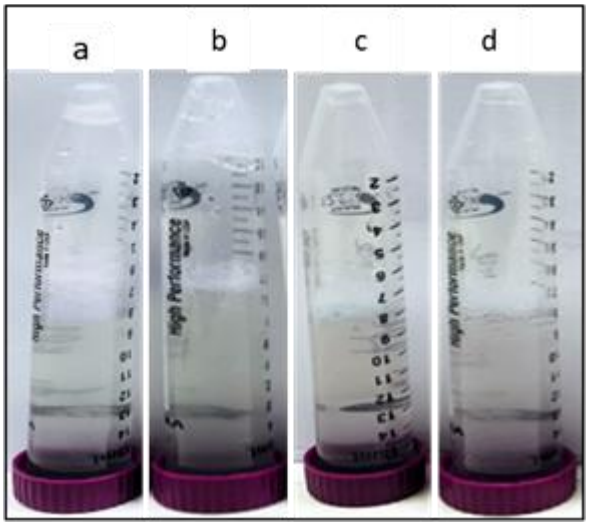


**Figure 22: Sample 3 washed in 10 mL a. $H_2O$ and b. HCl.**
**Sample 6 washed in 10 mL c. $H_2O$ and d. HCl.**

### 5.1.6. Adsorption capacity for Ca(II) ions

Ca(II) ions commonly present in fresh water sources are also attracted by carboxylic acid groups. On one hand, this constitutes competition to heavy metal ions adsorption, which in case of TEMPO-CNF filters is usually limited [49], but also opens up the opportunity to address another issue in drinking water quality: water hardness. The adsorption capacity of TEMPO-CNF filters for Ca(II) ions from aqueous solution was investigated by filtration experiments using a test solution of 2.5 mmol/L $CaCl_2$ (Figure 23).

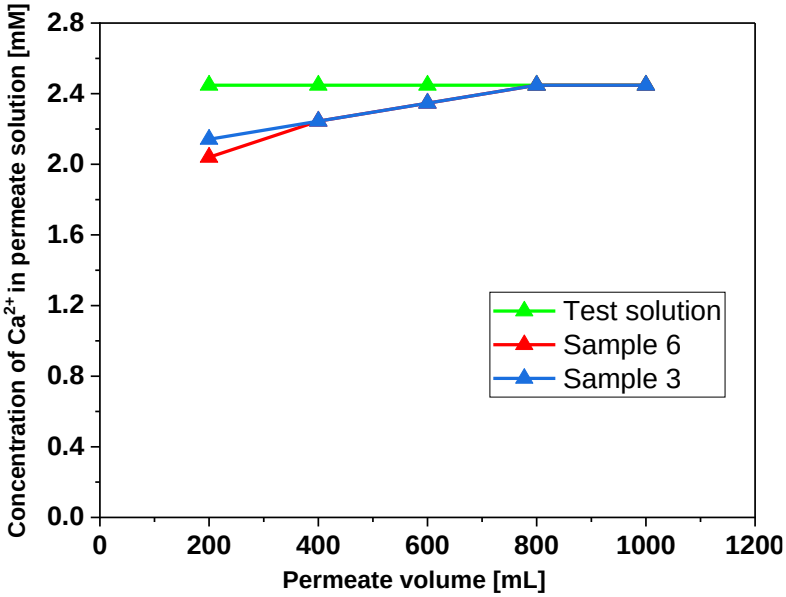


**Figure 23: Progression of continuous adsorption of Ca(II) ions.**

Similar to copper ions, more Ca(II) ions were adsorbed (63.6 mg/m$^2$) by sample 6 with a coat weight of 6.8 g/m$^2$ compared to sample 3 with 1.8 g/m$^2$ (54.1 mg/m$^2$) (Figure 24). Adsorption capacities of 8.8 and 30 mg/g were thus determined for sample 3 and sample 6, respectively. It was observed that the adsorption capacity increased with decreasing coat weight. The adsorption per area of samples 3 and 6 for Cu(II) ions were 75 and 128 mg/m$^2$, respectively, which was much higher adsorption compared to Ca(II) ions. Thus, hardly any negative impact by competitive adsorption of Ca(II) is expected for Cu(II) adsorption. Still, TEMPO-CNF filters exhibited appropriate adsorption capacity for Ca(II) ions, enabling the filters to reduce water hardness, which is an important factor for the quality of water. In comparision, pure TEMPO-oxidised phosphorylated nanopapers displayed an adsorption capacity of 91 mg/g and 70 mg/g for Ca(II) and Mg(II), respectively [50], which was higher but with the disadvantage of tremendously lower water permeance.

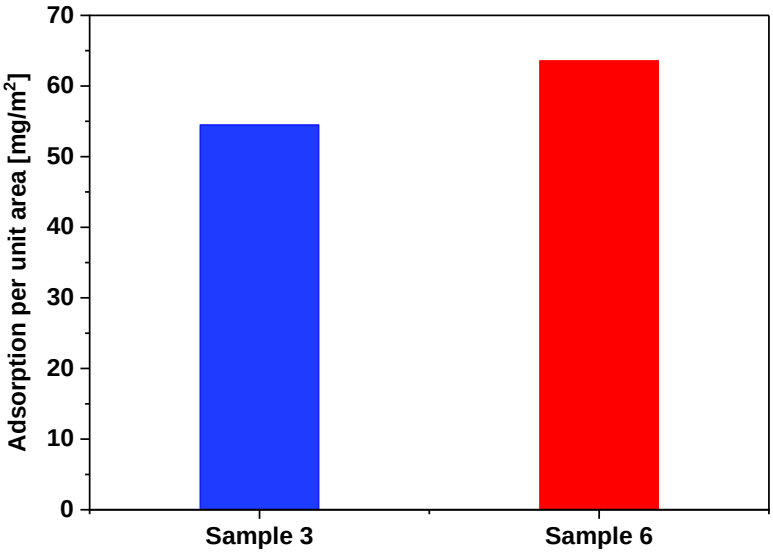


**Figure 24: Adsorption of Ca(II) ions [mg] per unit filter area [m$^2$].**

### 5.1.7. Mechanical properties of foam coated filters

The mechanical properties of foam coated TEMPO-CNF filters were analysed in wet and dry conditions. Stress-strain curves of the foam coated filters in both conditions are displayed in Figure 25. The strength, elastic modulus and strain to failure of each filter were determined from these stress-strain curves. The highest point of the stress-strain curve is the maximum tensile strength. It is a measure for the load a material can withstand before failure. The stiffness, or more precise the resistance to deformation, of a material is given by the Young's

moduli, which were calculated from the slope of the first linear region in the stress-strain curves. The elongation at break is the strain at maximum stress.

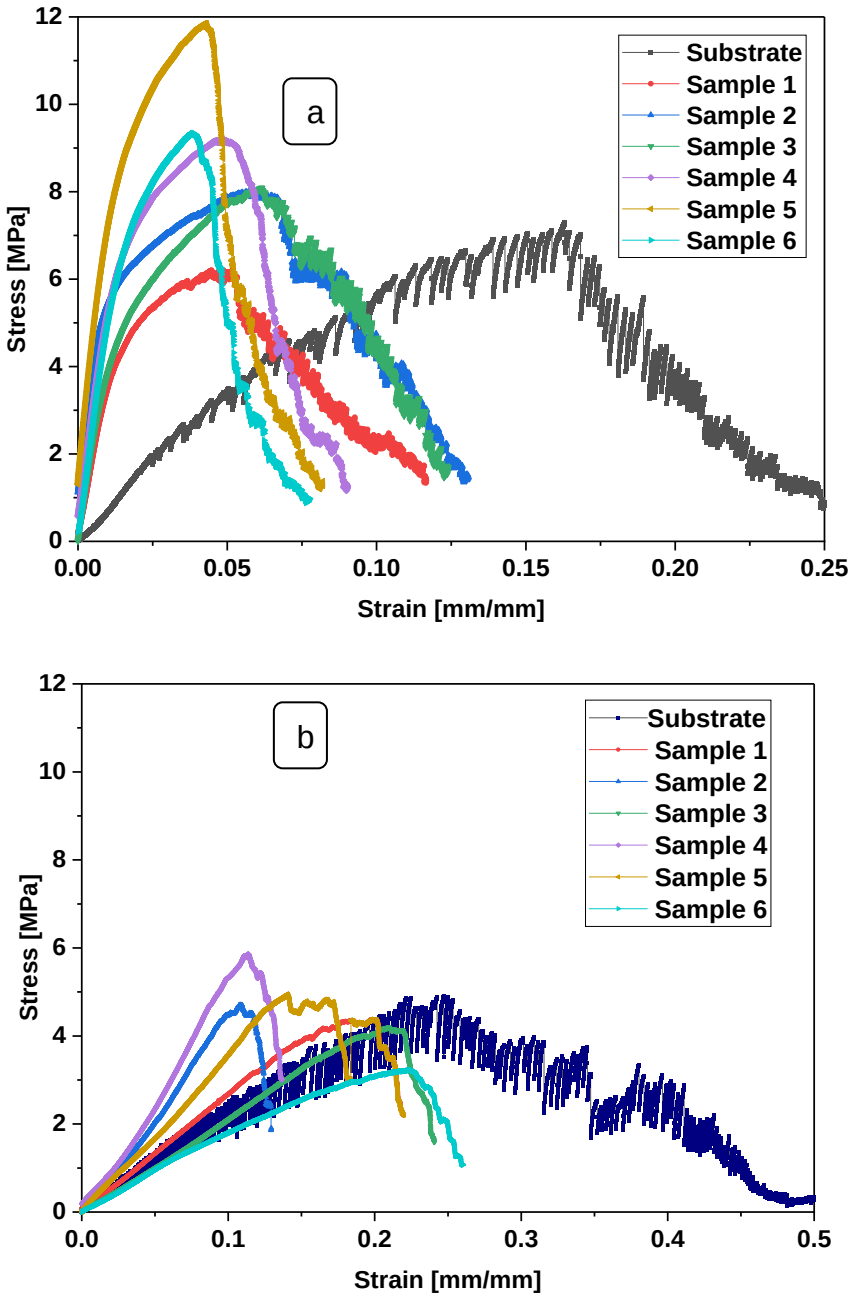


**Figure 25: Stress-strain curves of foam coated filters in dry (a) and wet (b) condition.**

The stress-strain curves exhibited an initial linear region, corresponding to the elastic deformation region of the foam coated TEMPO-CNF filters. Then the curves started to level off, indicating local plastic deformation, such as the pull-out or break of cellulose fibers in viscose filters. After the maximum tensile strength was passed, the stress was reduced continuously with prolonged elongation. This was due to the break of the TEMPO-CNF layer

on top or within the filters but the viscose fibers in the substrate still being loosely bond. Furthermore, coating with TEMPO-CNF, which behaves brittle, did reduce the tensile strain from 12 to 6 % in dry condition (Figure 25 a). Yet, the strain at maximum stress was influenced by the amount of TEMPO-CNF coated only to a minor extend. The Young's moduli and tensile strengths of foam coated TEMPO-CNF filters in dry condition increased from 40 MPa for the pure substrate to about 500 MPa for coated samples and from 7 to more than 12 MPa, respectively, (Figure 26). This indicates the reinforcement effect of the dry TEMPO-CNF on the viscose filters.

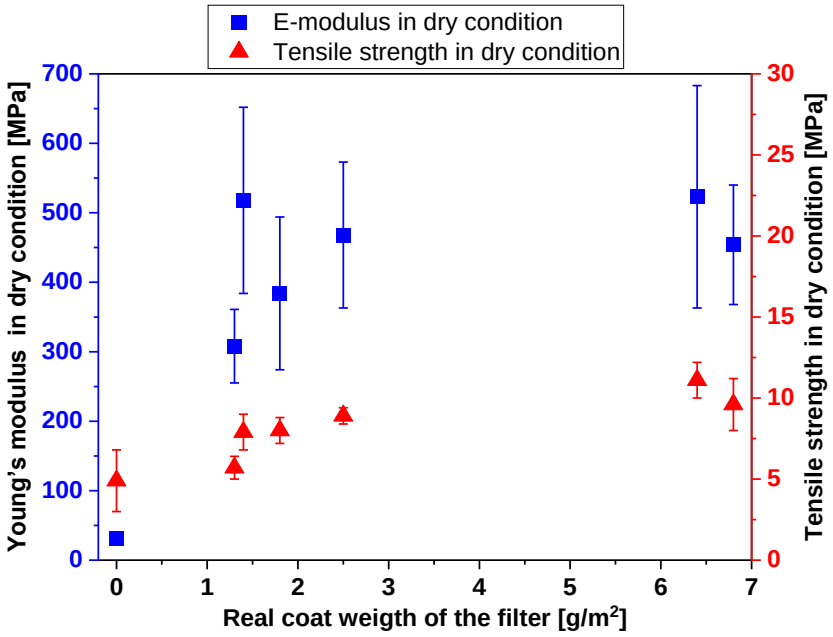


**Figure 26: E-modulus and tensile strength in dry condition vs. the coat weight of foam coated filters.**

The Young's moduli and tensile strengths of the wet substrate (21 and 4.4 MPa, respectively) and coated viscose filters (20.3 and 3.4, respectively) were identical within error (Figure 27). The TEMPO-CNF adsorbed water and became softer hence its reinforcement effect to the viscose filters vanished and the stiffness of the wet filters was controlled predominately by the viscose substrate. Still, in order to function as filter material these mechanical properties are considered sufficient, in the light that the coated filters had similar mechanical properties compared to the filter substrate.

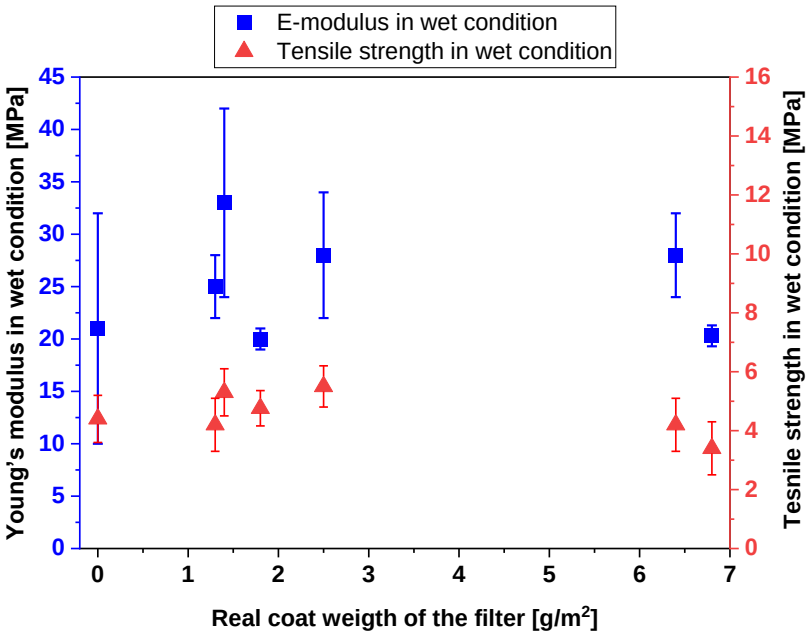


**Figure 27: E-modulus and tensile strength in wet condition vs. the coat weight of foam coated filters.**

## 5.2. Cast coated TEMPO-CNF filters

While the adsorption capacity of foam coated TEMPO-CNF filters was higher for lower coat weight, their areic adsorption was higher at higher coat weight. However, for foam coating the maximum coat weight is inherently limited by the volume of foam that can be applied on the substrate and collapsed. Thus, in order to increase the coat weight and hence the areic adsorption, TEMPO-CNF was also cast coated directly on the viscose substrate. By adjusting the thickness of the coating, the coat weight was controlled between 2.3 and 15.8 g/m$^2$, limited by the amount of water that could be removed during drying. Because of the high water content in the suspension, drying of the TEMPO-CNF coating could not be realised in continuous mode and the coated fabrics had to be kept in the drying zone for 20 min. During drying, the coated fabrics were fixed in the transverse direction to reduce the shrinkage. This impacted several parameters, such as the penetration and spreading of the suspension into the viscose fabric as well as the transverse shrinkage and stretching of the fabrics. Furthermore, the maximum coat weight was thus limited albeit significantly higher than for foam coating.

**Table 2: Coat weight and shrinkage of cast coated filters.**

| Code of sample | Set coat weight, [g/m$^2$] | Shrinkage | Real coat weight [g/m$^2$] |
|---|---|---|---|
| **Sample 7** | 1.3 | 0.07 | 2.3 |
| **Sample 8** | 2.7 | 0.10 | 5.7 |
| **Sample 9** | 2.7 | 0.10 | 7.8 |
| **Sample 10** | 5.8 | 0.10 | 5.2 |
| **Sample 11** | 8.5 | 0.08 | 14.0 |
| **Sample 12** | 8.5 | 0.02 | 14.6 |
| **Sample 13** | 10 | 0.13 | 15.8 |

As for foam coated filters a linear relationship between the coat weight and thickness of the filters was established, but with very small slope and an almost constant thickness of 200 to 250 µm (Figure 28) with a tendency to higher thicknesses at higher coat weight. This could be explained by TEMPO-CNF penetrating into the viscose substrates filling the pores rather than just being applied to the surface of the filters.

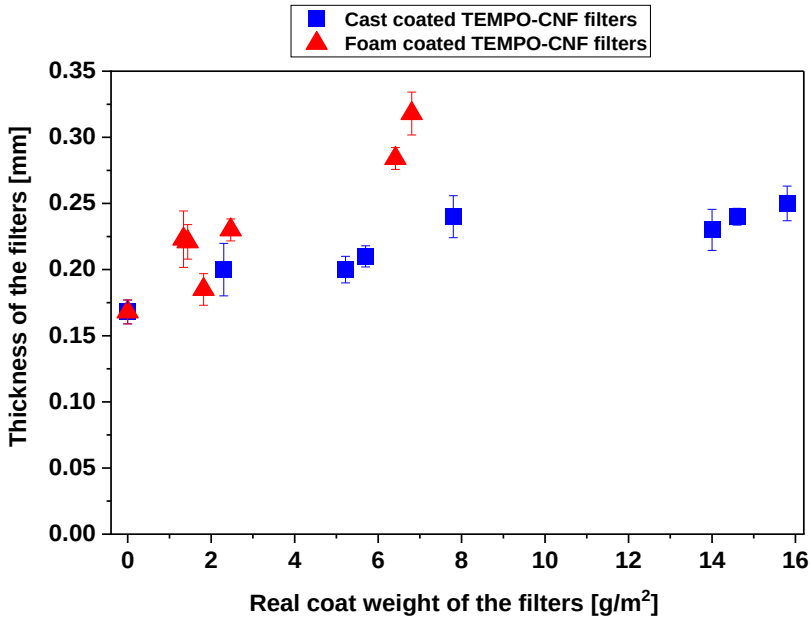


**Figure 28: Relationship between thickness and coat weight of cast coated filters.**

### 5.2.1. Morphology of cast coated filters

Figure 29 shows the surface and fiber morphologies of uncoated and cast coated filters with different coat weight. Non-woven fibers were visible on the surface of uncoated substrates. Compared to uncoated filters, the cast coated filters exhibited a thicker, denser and glossier top surface, especially for the filters with high coat weight. They showed a more compact, continuous and homogeneous surface structure. In particular sample 13 exhibited a denser and smoother surface as compared to samples 7-12, due to a high coat weight of 15.8 g/m$^2$. Furthermore, all cast coated filters exhibited a similar bottom surface as the uncoated substrate, indicating that also during cast coating TEMPO-CNF did not fully penetrate throughout the filter albeit thickness data suggest that it penetrated into the substrate to a certain extent.

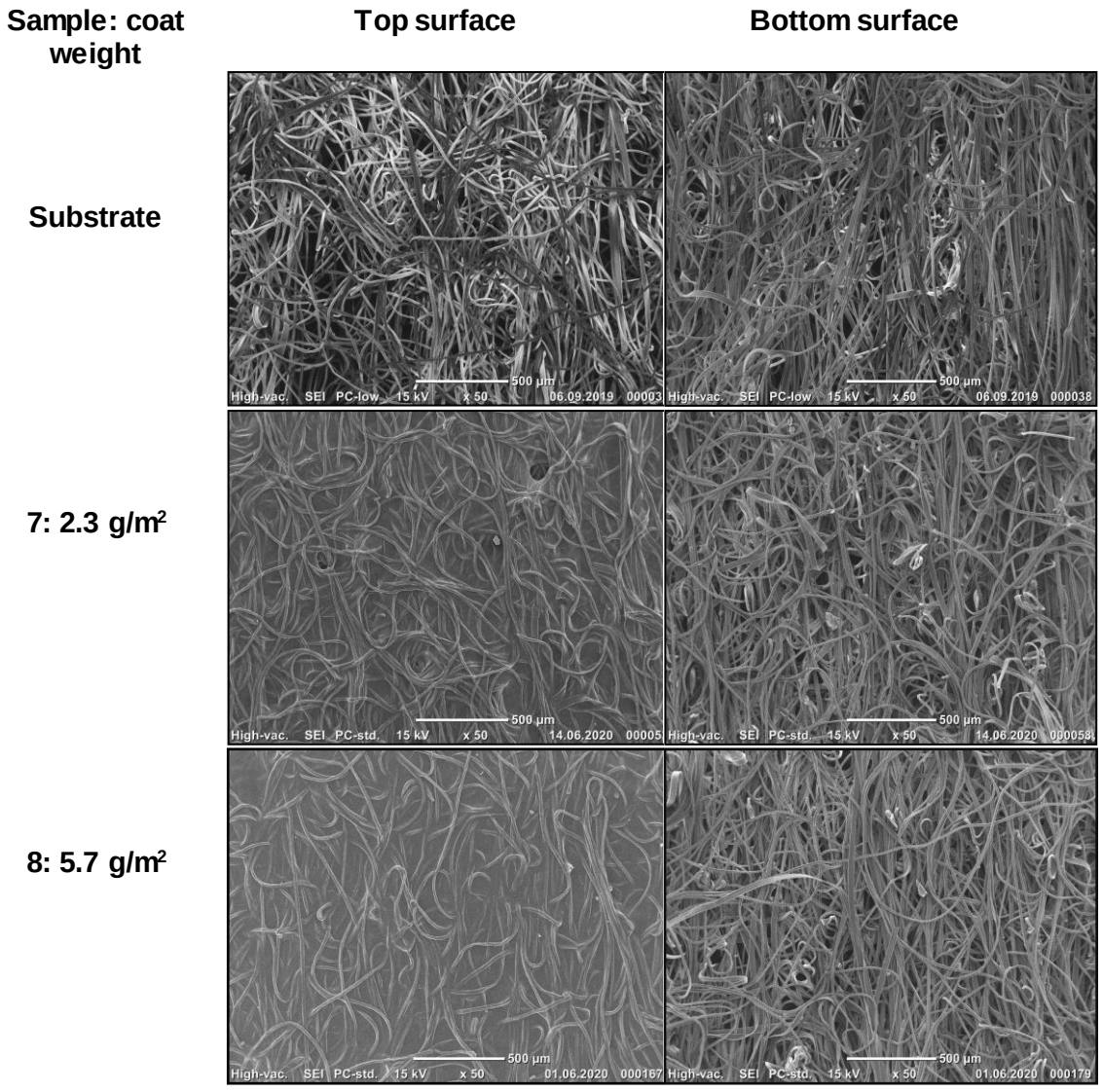

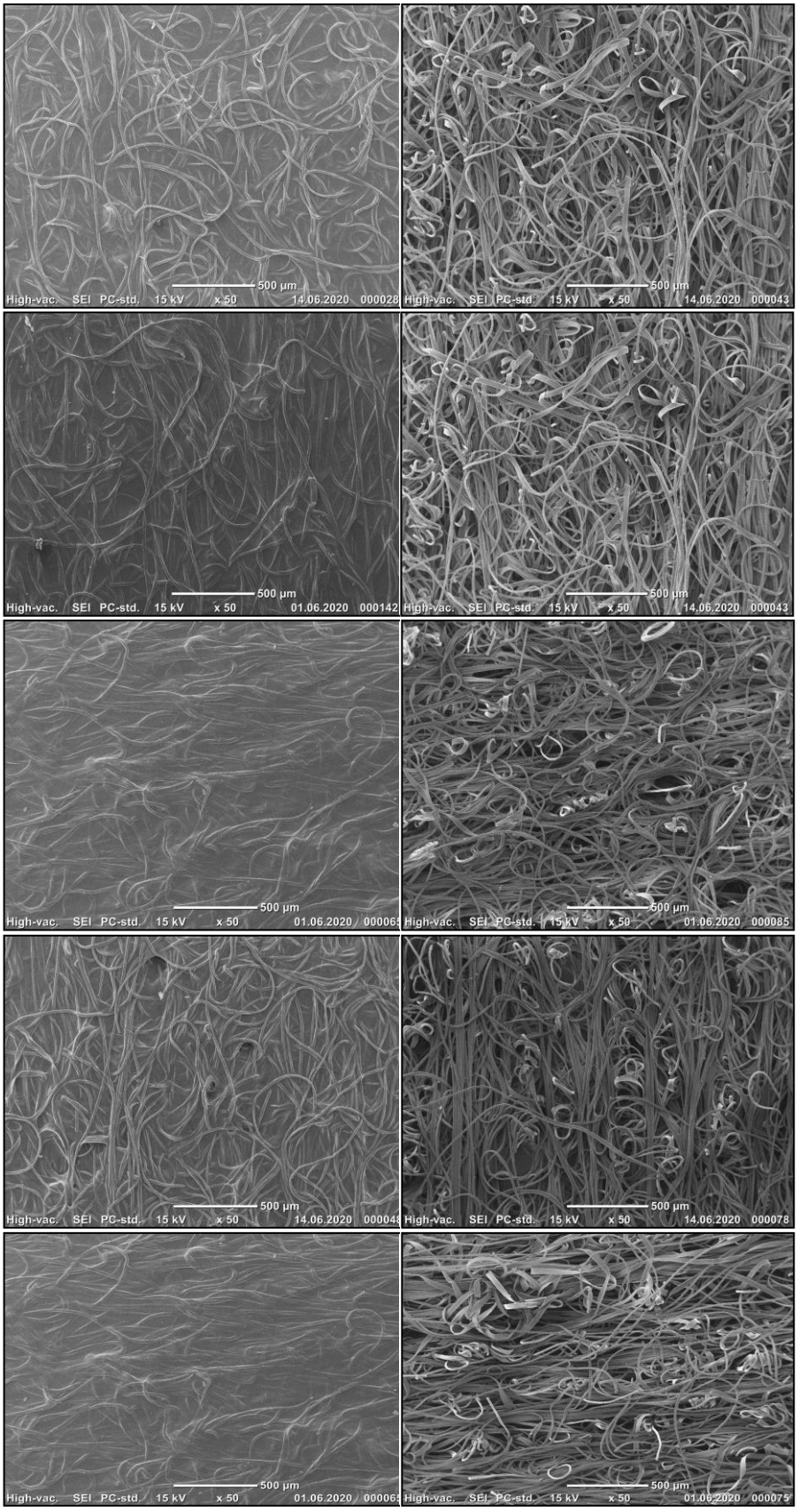


**Figure 29: SEM images of cast coated TEMPO-CNF filters.**

Cast coated TEMPO-CNF filters (Samples 13 and 7) are displayed in more detail in Figure 30. TEMPO-CNF was present as a very thin layer between fibers or coated on individual fibers (Figure 30a). However, occasional holes can be still observed in the coating layer, especially for samples with low coat weight (Figure 30b).

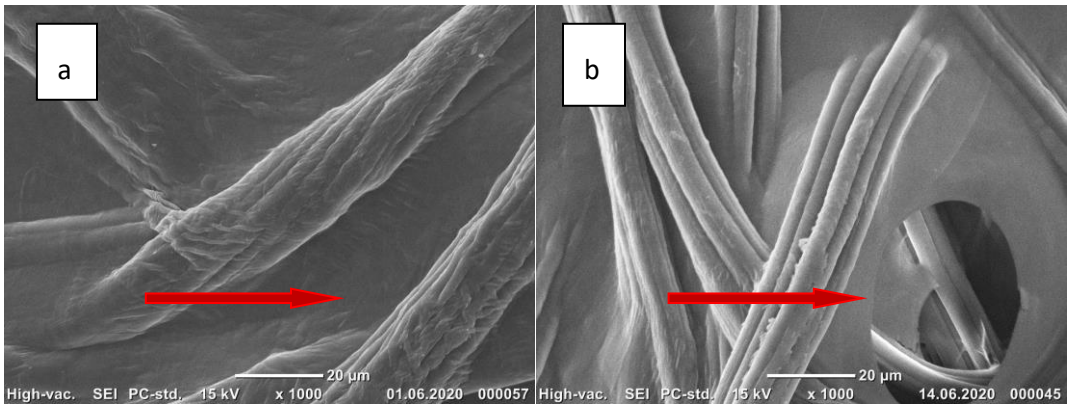


**Figure 30: SEM images of the surface of cast coated TEMPO-CNF filters at 1000× magnification, a. Sample 13 (15.8 g/m²) and b. Sample 7 (2.3 g/m²). Red arrows indicate the surface of cast coated TEMPO-CNF filters.**

### 5.2.2. Pure water permeance

Compared to the uncoated substrates that exhibited a permeance of 420000 L / m² h MPa (at 0.2 bar), the cast coated filters had reduced permeances of 380000 to 100000 L / m² h MPa (at 0.2 bar). The permeance significantly decreased as the coat weight increased (Figure 31). Furthermore, the cast coated filters exhibited substantially lower permeance than foam coated filters (Figure 32). This can be explained by higher coat weights of cast coated filters and the resulting denser layer on top of the substrate, which functions as a barrier resisting the water to pass through.

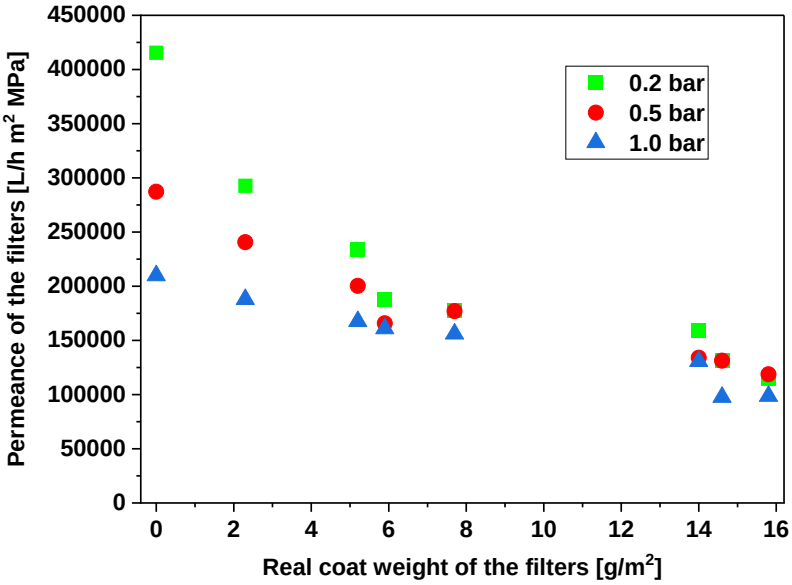


**Figure 31: Water permeance vs. real coat weight of cast coated filters.**

The permeance of most of the filters decreased as backpressure increased, which can be explained by filter compaction caused by the backpressure (Figure 32). However, at high coat weights and due to the denser layer this effect was reversed for 0.2 bar were apparently too little to effectively push the water through the filters. Still, permeances of more than 100 000 L / m² h MPa are considered sufficient for water filtration applications.

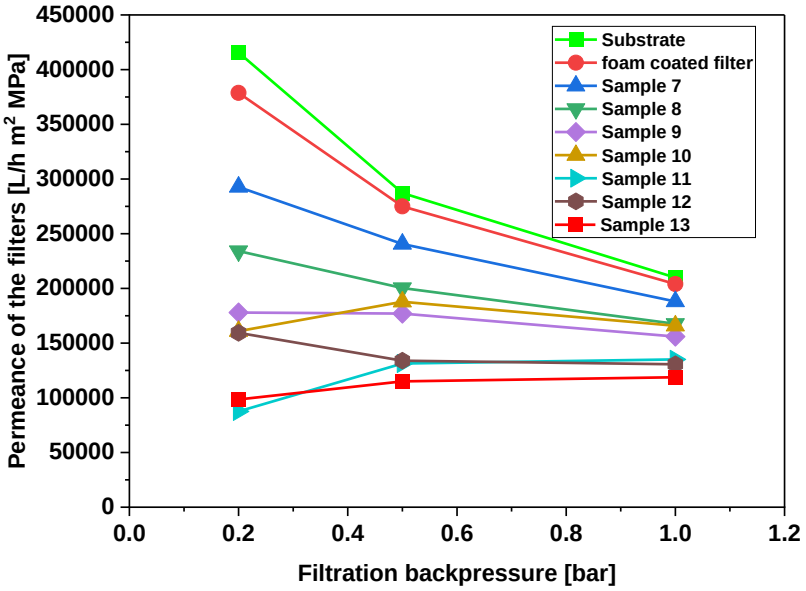


**Figure 32: Water permeance vs. backpressure.**

### 5.2.3. Adsorption capacity for Cu(II) ions

Cu(II) adsorption of cast coated filters was analysed using the same method as for foam coated filters described above. It was noted that the feed solutions passed through the cast coated filters much slower (1 to 2 min) compared to foam coated filters because of the higher coat weight and their dense layer on top of the filters. Furthermore, for some filters saturation was reached after a higher number of test cycles, i.e. volume of the feed solution filtered (Figure 33) indicating a high absolute number a Cu(II) ions having been adsorbed compared to foam coated filters.

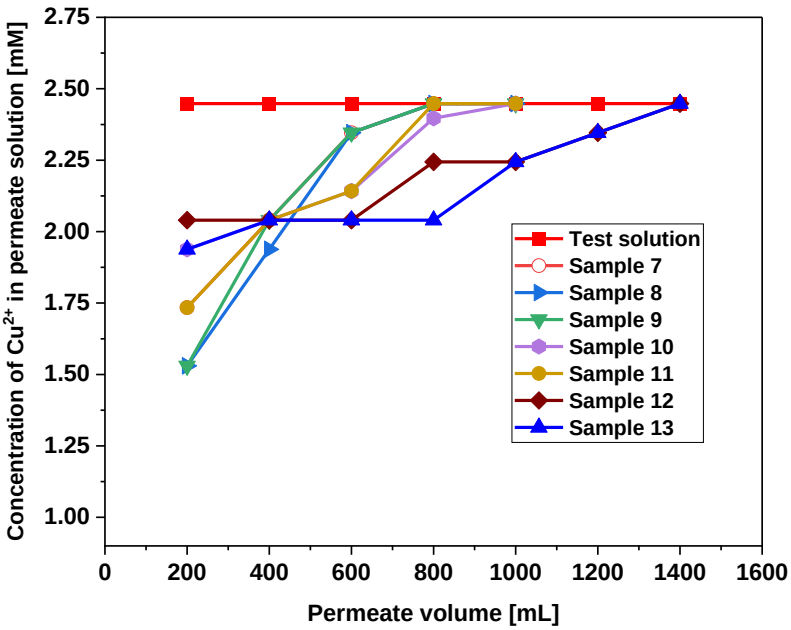


**Figure 33: Concentration of Cu(II) ions in permeate solution vs. permeate volume for cast coated TEMPO-CNF filters.**

After filtration, the cast coated TEMPO-CNF filters were coloured blue, indicating the adsorption of Cu (II) ions onto the filter surface. The values of the areic adsorption and adsorption capacities of the foam and cast coated filters with various coat weights are shown in Figures 34 and 35. Compared to the substrate and foam coated filters, the cast coated filters exhibited higher areic adsorption of up to 280 mg/m$^2$, due to the larger surface area formed by the deeper penetration of the coating (Figure 34).

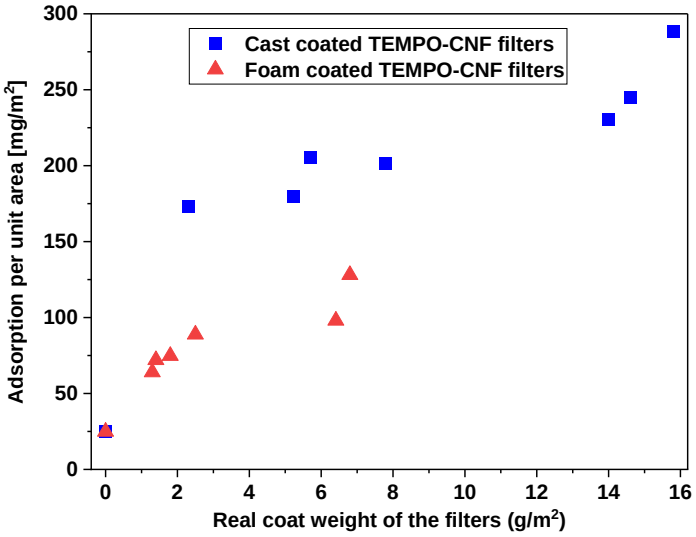


**Figure 34: Adsorption per unit filter area [m²].**

Similar to foam coated filters there was a linear relationship between areic adsorption and coat weight up to 15.8 g/m² with TEMPO-CNF filters with a higher amount of carboxyl groups exhibiting higher Cu(II) adsorption [13]. Increasing the number of free carboxyl groups on the surface of the cellulose chains improves the retention of divalent ions from aqueous solution [1]. On the other hand, adsorption capacity per coat weight decreased with increasing coat weight (Figure 35), indicating that the adsorption preferentially took place at the surface of the filters. Higher adsorption at same coat weights for cast coated filters compared to foam coated filters could be ascribed to longer residence and contact times of Cu(II) ions caused by the lower permeance.

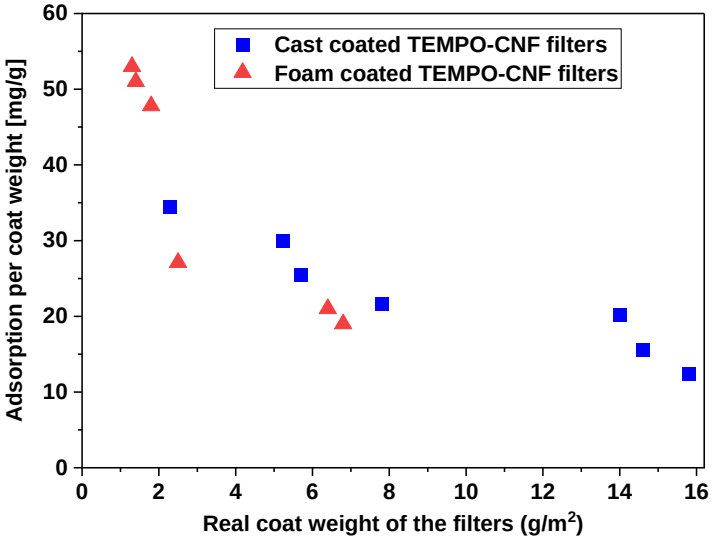


**Figure 35: Adsorption as function of coat weight for foam and cast coated TEMPO-CNF filters.**

### 5.2.4. Regeneration and reuse of cast coated filters

Figure 36 shows the results of regeneration and reuse experiments with cast coated TEMPO-CNF filters. The optimised regeneration process was applied and filters soaked in HCl at pH = 2 for 2 h. More than 90% of Cu(II) were recovered from the filters during the first washing cycle. The amount desorbed by a second washing cycle was almost zero, further confirming that the copper ions were already mostly removed from the cast coated TEMPO-CNF filters during the optimised regeneration procedure. Furthermore, a high amount of Cu(II) ions could be re-adsorbed (186 mg/m$^2$ and 202 mg/m$^2$), corresponding to 76 % and 74 % of the original amount adsorbed for the regenerated cast coated filters samples 11 and 13, respectively (Figure 36). Similar to foam coated filters this result shows that the cast coated filters could be regenerated with HCl treatment and applied as absorbents with high reusability. Lower desorption from cast coated filters compared to foam coated filters could be explained by a denser structure of the coating from which desorption is slightly more hindered.

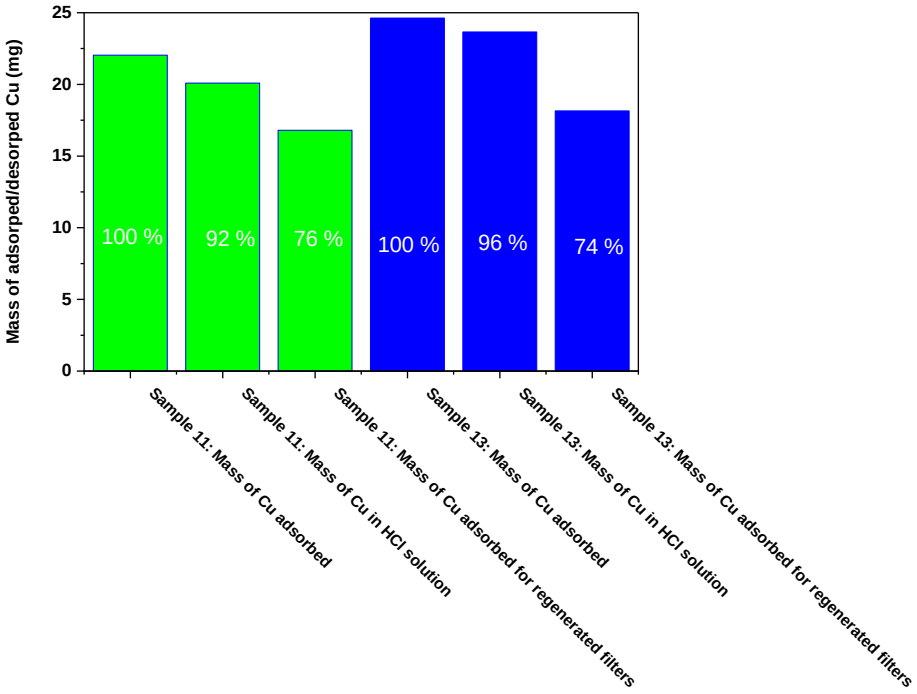


**Figure 36: Desorption and adsorption performance of (regenerated) cast coated TEMPO-CNF filters.**

### 5.2.5. Leaching of fiber fragments

Leaching of substrate fiber fragments from the cast coated filters was investigated. After shaking filters with HCl or $H_2O$, respectively, the filters were removed from solutions. Opposed to foam coated filters, no foam was observed on top of the washing solutions, due to the absence of surfactant in the formulations of the cast coated filters. However, the solution became cloudy, indicating that fibre fragments might be released from the filter during shaking (Figure 37).

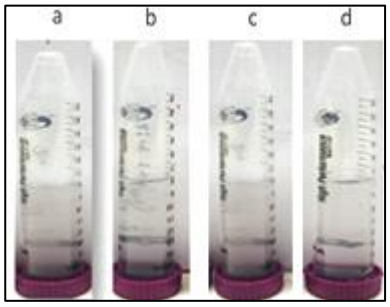


**Figure 37: Sample 11 in 10 mL a. $H_2O$ and b. HCl, Sample 13 in 10mL c. $H_2O$ and d. HCl.**

### 5.2.6. Mechanical properties of cast coated filters

Mechanical properties of the cast coated TEMPO-CNF filters were analysed both in wet and dry conditions. The stress-strain curves of the average of seven tensile tests are shown in Figure 38. The stress-strain curves had a linear region within a strain range from 0 to 0.01 in dry and 0 to 0.1 in wet conditions, respectively, corresponding to the elastic deformation region of the cast coated TEMPO-CNF filters. After that, the curves began to flatten, indicating local plastic deformation, such as the pull-out or breaking of cellulose fibers in filters. This plastic deformation continued until the stress reached maximum, indicating maximum tensile stress. The uncoated sample showed a much higher yield point of 15 and 24 %, respectively, compared to cast coated TEMPO-CNF filters in both dry and wet conditions, respectively. This could be explained by TEMPO-CNF coating hindering the elongation of the viscose fiber network. A higher elongation at yield point was detected for all samples in wet condition than in dry condition.

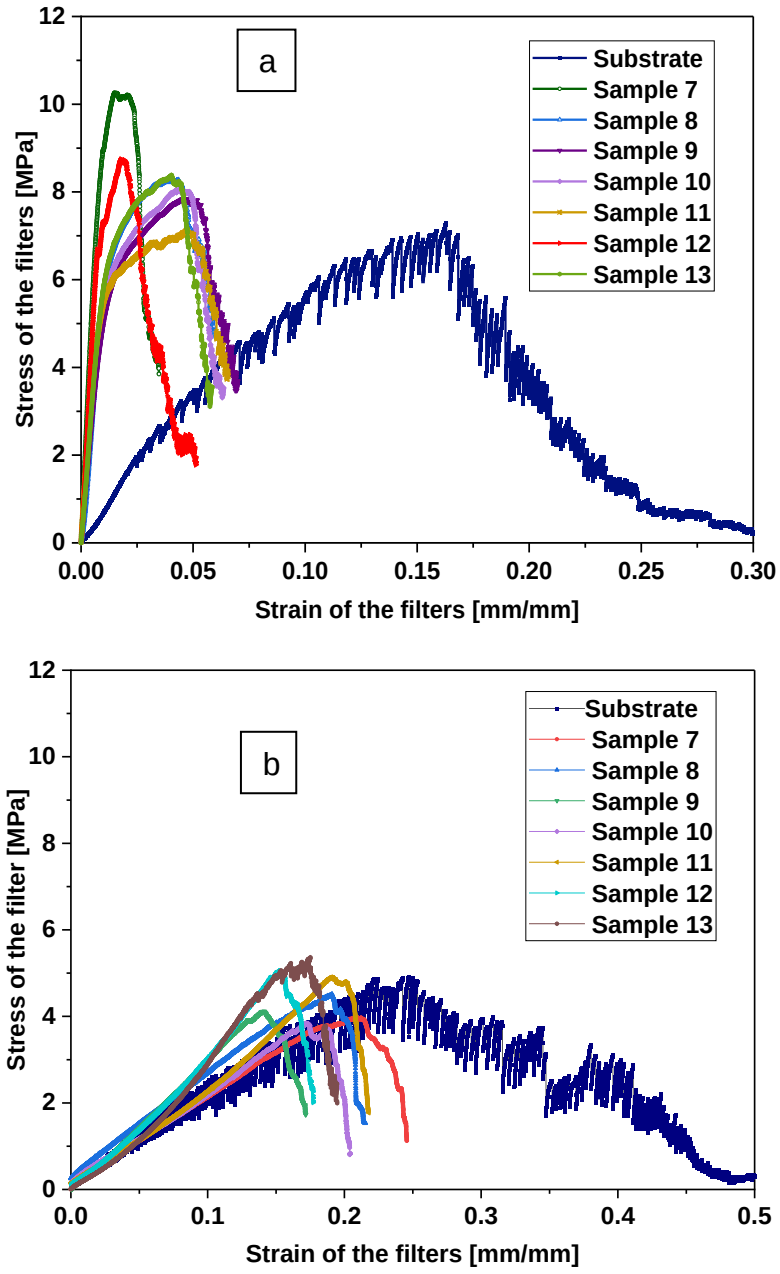


**Figure 38: Stress-strain curves of cast coated filters in dry (a) and wet (b) condition.**

Young's moduli and tensile strengths of uncoated and cast coated filters in dry conditions are shown in Figure 39. The coating increased both Young's moduli and tensile strengths from 7 to 10 and 500 to 1000 MPa, respectively. The Young's moduli of cast coated TEMPO-CNF filters in dry condition were between 40 and 1000 MPa. This means that the stiffness/resistance to deformation of the filter was improved by cast coating, but the strength was on the same level.

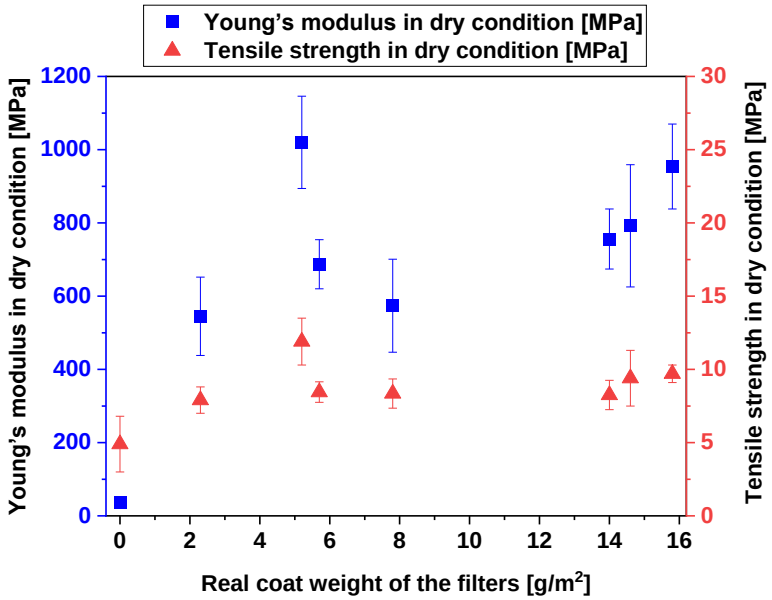


**Figure 39: E-modulus and tensile strength of cast coated filters in dry condition.**

The Young's moduli and tensile strengths of wet uncoated and coated viscose filters were identical within error (Figure 40), which was already observed for dry foam coated filters. Furthermore, all foam and cast coated samples had tensile strengths of more than 4 MPa in wet conditions, which was basically equivalent to the uncoated sample (4.4 MPa).This could be explained by the TEMPO-CNF layer absorbing water and thus softening. Hence, there was hardly any reinforcing effect by the coating.

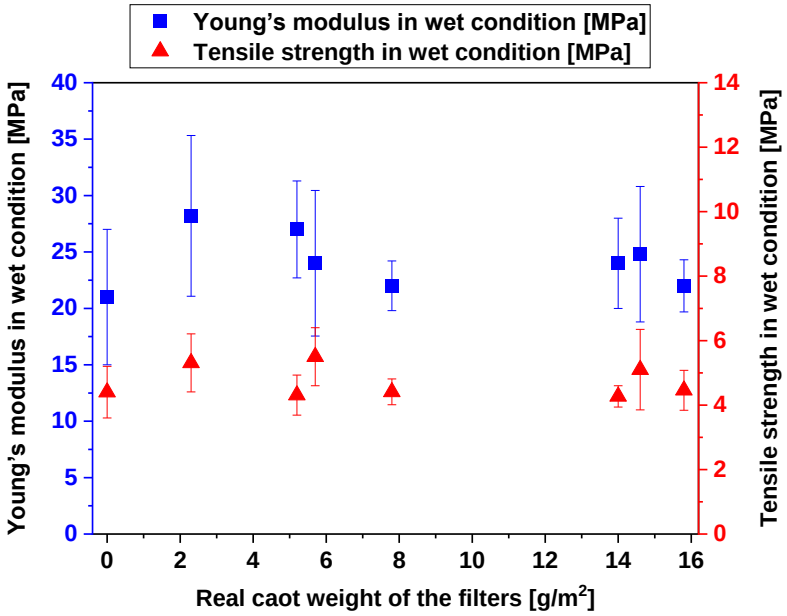


**Figure 40: E-modulus and tensile strength of cast coated filters in wet condition.**

## 6. Conclusions

This study demonstrates the potential of foam and cast coated TEMPO-CNF filters produced in pilot scale for the removal of metal ions, such as Cu(II), from aqueous solution. TEMPO-CNF were coated on viscose filters by using two different coating approaches, foam and cast coating, to manufacture a flat filter containing TEMPO with different coat weights. The real coat weight of foam coated filters was between 1.3 and 6.8 g/m$^2$ whereas it was between 2.3 and 15.8 g/m$^2$ for cast coated filters. SEM images confirmed the presence of TEMPO-CNF on the surface of the viscose substrate. The TEMPO-CNF coating was shown as thin layers on the surface of single cellulose fibers or between fibers. A dense coating layer was found for the TEMPO-CNF filters with high coat weights. The performance of TEMPO-CNF filters was evaluated in terms of their water permeance as well as adsorption of Cu(II) ions. It was found that the efficiency of TEMPO-CNF filters was related to their coat weight. Cast coated filters showed a higher areic adsorption of up to 280 mg/m$^2$ for Cu(II) compared to foam coated filters (25 to 128 mg/m$^2$) due to their higher coat weight. However, foam coated filters had a higher adsorption capacity of 19 to 52 mg/g than cast coated filters (10 to 35 mg/g), indicating higher efficiencies of the adsorption process. Furthermore, both types of TEMPO-CNF filters exhibited much higher absorption capacity for Cu(II) as well as Ca(II) ions compared to the uncoated substrate. This was explained by the high amount of carboxyl groups on the surface of filters. The available $COO^-$ sites allowed for the adsorption of metal ions. Adsorption of Ca(II) ions was much lower than for Cu(II) ions, indicating that Cu(II) ions will be preferentially adsorbed under competitive conditions but reasonably high to facilitate reduction of permanent water hardness, which is important for improving water quality. The permeance of foam and cast coated TEMPO-CNF filters was kept at about 330000 to 430000 L / m$^2$ h MPa and 100000 to 380000 L / m$^2$ h MPa at 0.2 bar, respectively. Such high water flux benefits the application of the filters by allowing the treatment of large quantities of water in short time. Furthermore, up to 99 % of Cu (II) was recovered from the TEMPO-CNF filters by using optimised regeneration conditions utilizing HCl. A high amount of re-adsorption of more than 70% remained for the regenerated foam and cast coated TEMPO-CNF filters. Thus it was concluded that foam and cast coated TEMPO-CNF filters have high potential for use in filtration as well as the adsorption of water contaminants including heavy metal ions, as shown for Cu(II).

## References

[1] **Nuria Fiol, Matias Vasquez, Miguel Pereira, Quim Tarre, Pere Mutje and Marc Delgado Aguila.** TEMPO-oxidised cellulose nanofibers as potential Cu(II) adsorbent for wastewater treatment. Cellulose, vol. 26, 2019, pp. 903-916.

[2] **Ilka Gehrke, Andreas Geiser and Annette Somborn-Schulz**. Innovations in nanotechnology for water treatment. Nanotechnology, Science and Applications, vol. 8, 2015, pp. 1-17.

[3] **Andreas Mautner.** Nanocellulose water treatment membranes and filters: A review. Polymer International, vol. 69, 2020, pp. 741-751.

[4] **United Nations World Water Assessment Programme.** The United Nations World Water Development Report. Wastewater, 2017, pp. 1-17.

[5] **Sabino De Gisi, Giusy Lofrano, Mariangela Grassi and Michele Notarnicola.** Characteristics and adsorption capacities of low-cost sorbents for wastewater treatment: A review. Sustainable Materials and Technologies, vol. 10, 2016, pp. 10-40.

[6] **Jaimin Pandya.** Nanofiltration for Recovery of Heavy Metal from Waste Water. Chemical Engeering Journal, vol. 10, 2010, pp. 1-20.

[7] **Sabu Thomas, Daniel Pasquini, Shao Yuan Leu and Deepu Gopakumar.** Nanoscale Materials in Water Purification. Materials science, vol. 1, 2018, pp. 383-430.

[8] **Amita Sharmaa, Manisha Thakura, Munna Bhattacharyaa and Tamal Mandalb.** Commercial application of cellulose nano-composites – A review. Biotechnology Reports, vol. 4, 2019, pp. 1-15.

[9] **Zoheb Karim, Minna Hakkalahi, Tekla Tammelin and Aji Mathew.** In situ TEMPO surface functionalisation of nanocellulose membranes for enhanced adsorption of metal ions from aqueous medium. RSC Advances, vol. 7, 2017, pp. 5232-5241.

[10] **Akira Isogai, Tsuguyuki Saito and Hayaka Fukuzumi.** TEMPO-oxidised cellulose nanofibers. Nanoscale, vol. 3, 2011, pp. 71-85.

[11] **Monisha Jaishankar, Tenzin Tseten, Naresh Anbalagan, Blessy Mathew and Krishnamurthy Beeregowda.** Toxicity, mechanism and health effects of some heavy metals. Interdisciplinary Toxicology, vol. 7:2, 2014, pp. 60-72.

[12] **Vhahangwele Masindi and Khathutshelo Muedi.** Environmental Contamination by Heavy Metals. Journal of Enviromental Sciences, vol. 10:5, 2018, pp. 115-133.

[13] **Peng Liu, Beatriz Garrido, Kristiina Oksman and Aji Mathew.** Adsorption isotherms and mechanisms of Cu(II) sorption onto TEMPO-mediated oxidised cellulose nanofibers. RSC Advances, vol. 6, 2016, pp. 107759-107767.

[14] **Andreas Mautner, Yosi Kwaw, Kathrin Weiland, Mlando Mvubu, Anton Botha, Maya Jacob John, Asanda Mtibe, Gilberto Siqueira and Alexander Bismarck.** Natural fibre-nanocellulose composite filters for the removal of heavy metal ions from water. Industrial Crops and Products, vol. 133, 2019, pp. 325-332.

[15] **Abdel Raof and Abdul Raheim.** Removal of Heavy Metals from Industrial Waste Water by Biomass-Based Materials: A Review. Journal of Pollution Effects and Control, vol. 5:1, 2017, pp. 1-17.

[16] **Marton Czikkely, Eva Neubauer, Ilona Fekete, Prespa Ymeri and Csaba Fogarassy.** Review of Heavy Metal Adsorption Processes by Several Organic Matters from Wastewaters. Water, vol. 10, 2018, pp. 1-15.

[17] **Anitha Georgy Varghese, Sherely Annie Paul and Asha Latha Mettla.** Remediation of heavy metals and dyes from wastewater using cellulose-based adsorbents. Environmental Chemistry Letters, vol. 17, 2019, pp. 867-877.

[18] **Subhas Sarkar and Subhendu Adhikari.** Adsorption Technique for Removal of Heavy Metals from Water and Possible Application in Wastewater-Fed Aquaculture. Natural Science, vol. 10, 2018, pp. 235-250.

[19] **Arezoo Azimi, Ahmad Azari, Mashallah Rezakazemi and Meisam Ansarpour.** Removal of Heavy Metals from Industrial Wastewater: A Review. Chemical Biomolecular Engeering, vol. 4:1, 2017, pp. 37-59.

[20] **Madhu Agarwal and Kulvir Singh.** Heavy metal removal from wastewater using various adsorbents: A review. Journal of Water Reuse and Desalination, vol. 7:4, 2017, pp. 387-419.

[21] **Abhishek Kardam, Kumar Rohit Raj, Shalini Srivastava and Muktabh Mayank Srivastava.** Nanocellulose fibers for biosorption of cadmium, nickel and lead ions from aqueous solution. Clean Technologies and Environmental Policy, vol. 16, 2014, pp. 385-393.

[22] **Katrina Pui Yee Shak, Yean Ling Pang and Shee Keat Mah.** Nanocellulose: Recent advances and its prospects in environmental remediation. Journal of Nanotechnology, vol. 9, 2018, pp. 2479-2498.

[23] **Patchiya Phanthong, Prasert Reubroycharoen, Xiaogang Hao, Guangwen Xu, Abuliti Abudula and Guoqing Guan.** Nanocellulose: Extraction and application. Carbon Resources Conversion, vol. 1, 2018, pp. 32-43.

[24] **Rushdan Ahmad Ilyas, Salit Mohd Sapuan, Mahmud Siti Nur Atikah, Rushdan Ibrahim, Mohamad Hazrol, Muhammad Harussani Moklis, Tarique Jamal, Ahmed Nazrin and Syafig Mohammad Ridzuan.** Natural Fibre: A promising source for the production of nanocellulose. Natural Polymer Composites, vol. 7, 2020, pp. 2735-1246.

[25] **Amita Sharma, Manisha Thakur, Munna Bhattacharya, Tamal Mandal and Saswata Goswami**. Commercial application of cellulose nano-composites – A review. Biotechnology Reports, vol. 21, 2018, pp. 1-15.

[26] **Sanna Hokkanen, Amit Bhatnagar, Eveliina Repo, Song Lou and Mike Sillanpä**. Calcium hydroxyapatite microfibrillated cellulose composite as a potential adsorbent for the removal of Cr(IV) from aqueous solution. Chemical Engeering Journal, vol. 283, 2016, pp. 445-452.

[27] **Manali Banerjee, Sisira Saraswatula, Anna Williams and Blair Brettman.** Effect of Purification on Commercially Available Cellulose Nanocrystal Properties and TEMPO Oxidation. Green Synthesis and Functionalisation of Cellulose Fibers, vol. 8:698, 2020, pp. 1-14.

[28] **Han Qiao, Yanmei Zhou, Fang Yu, Enze Wang, Yinghao Min, Qi Huang, Lanfang Pang and Tongsen Ma.** Effective removal of cationic dyes using carboxylate-functionalised cellulose nanocrystals. Chemosphere, vol. 141, 2015, 297-303.

[29] **Alexis Wells Carpenter, Charles-François de Lannoy and Mark Robert Wiesner.** Cellulose Nanomaterials in Water Treatment Technologies. Environmental Science and Technology, vol. 49, 2015, pp. 5277-5287.

[30] **Hugo Voisin, Lennart Bergström, Peng Liu and Aji Mathew.** Nanocellulose-Based Materials for Water Purification. Nanomaterials, vol. 7:57, 2017, pp. 1-18.

[31] **Norhene Mahfoundhi and Sami Boufi**. Nanocellulose as a novel nanostructured adsorbent for environmental remediation: A review. Cellulose, vol. 24, 2017, pp. 1171-1197.

[32] **Dong Wang.** A critical review of cellulose-based nanomaterials for water purification in industrial processes. Cellulose, vol. 26, 2019, pp. 687-701.

[33] **Nataraj Sanna Kotrappanavar, Hosamani Kallappa Mahadevappa and Tejral Aminabhavi.** Nanofiltration and reverse osmosis thin film composite membrane module for the removal of dye and salts from the simulated mixtures. Desalination, vol. 249, 2009, pp. 12-17.

[34] **Dinesh Kumar Patel, Sayan Deb Dutta and Ki Taek Lim.** Nanocellulose-based polymer hybrids and their emerging applications in biomedical engineering and water purification. RSC Advances, vol. 9, 2019, pp. 19143-19162.

[35] **Kristiina Oksman, Aji Mathew, Pia Ovintus, Alexander Bismarck, Orlando Rojas and Mohini Sain**. Handbook of Green Materials: Processing Technologies, Properties And Applications. World Scientific, London, vol. 4, 2014.

[36] **Alexander Tucker Schwartz and Robin Garrell.** Simple Preparation and Application of TEMPO-coated $Fe_3O_4$ Superparamagnetic Nanoparticles for Selective Oxidation of Alcohols. Chemistry A European Journal, vol. 16, 2010, pp. 12718-12726.

[37] **Famei Qin, Zhiqiang Fang, Jie Zhou, Chuan Sun, Kaihuang Chen, Zixian Ding, Guanhui and Xueqing Qiu**. Efficient Removal of $Cu^{2+}$ in Water by Carboxymethylated Cellulose Nanofibrils: Performance and Mechanism. Biomacromolecules, vol. 12, 2019, pp. 1-11.

[38] **Moe Wakabayashi, Shuji Fujisawa, Tsuguyuki Saito and Akira Isogai.** Nanocellulose Film Properties Tunable by Controlling Degree of Fibrillation of TEMPO-Oxidised Cellulose. Polymer Chemistry, vol. 8:37, 2020, pp. 1-19.

[39] **Xiankui Sang, Chengrong Qin, Zhangfa Tong, Song Kong, Zhuan Jia, Guangcong Wan and Xinliang Liu.** Mechanism and kinetics studies of carboxyl group formation on the surface of cellulose fiber in a TEMPO-mediated system. Cellulose, vol. 24, 2017, pp. 2415-2425.

[40] **Akira Isogai, Tuomas Hänninen, Shuji Fujisawa and Tsuguyuki Saito.** Review: Catalytic Oxidation of cellulose with nitroxyl radicals under aqueous conditions. Progress in Polymer Science, vol. 86, 2018, pp. 122-148.

[41] **Chih Feng Huang, Jem Kun Chen, Tzung Yung Tsai, Ya An Hsieh and Kun-Yi Andrew Lin**. Dual-functionalised cellulose nanofibrils prepared through TEMPO mediated oxidation and surface-initiated ATRP. Polymer, vol. 72, 2015, pp. 395-405.

[42] **Sharon Olivera, Handanahally Basavarajaiah Muralidhara, Krishna Venkatesh, Vijay Kumar Guna, Keshavanarayana Gopalakrishna and Yogesh Kumar.** Potential applications of cellulose and chitosan nanoparticles/composites in wastewater treatment: A review. Carbohydrate Polymers, vol. 153, 2016, pp. 600-618.

[43] **Moe Wakabayashi, Shuji Fujisawa, Tsuguyuki Saito and Akira Isogai.** Nanocellulose Film Properties Tunable by Controlling Degree of Fibrillation of TEMPO-Oxidised Cellulose. Polymer Chemistry, vol. 8:37, 2020, pp. 1-19.

[44] **Andreas Mautner, Thawanrat Kobkeatthawin, Florian Mayer, Christof Plessl, Selestina Gorgieva, Vanja Kokol and Alexander Bismarck.** Rapid Water Softening with TEMPO-Oxidised/Phosphorylated Nanopapers. Nanomaterials, vol. 9:136, 2019, pp. 1-18.

[45] **Deepu Gopakumar, Vishnu Arumughan, Daniel Pasquini, Shao-Yuan Leu, Abdul Khalil and Sabu Thomas.** Nanocellulose-Based Membranes for Water Purification. Micro and Nano Technologies, vol. 27, 2019, pp. 59-85.

[46] **Peng Liu, Kristiina Oksman and Aji Mathew.** Surface adsorption and self-assembly of Cu(II) ions on TEMPO-oxidised cellulose nanofibers in aqueous media. Colloid and Interface Science, vol. 464, 2016, pp. 175-182.

[47] **Houssine Sehaqui, Uxua Perez de Larraya, Peng Liu, Numa Pfenninger, Aji Mathew, Tanja Zimmermann and Philippe Tingaut.** Enhancing adsorption of heavy metal ions onto biobased nanofibers from waste pulp residues for application in wastewater treatment. Cellulose, vol. 21, 2014, pp. 2831-2844.

[48] **Kennedy Chibuzor Onyelowe, Duc Bui Van, Obiekwe Ubachukwu, Charles Ezugwu, Bunyamin Salahudeen, Manh Nguyen Van, Chijioke Ikeagwuani, Talal Amhadi, Felix Sosa, Wei Wu , Thinh Ta Duc, Adrian Eberemu, Tho Pham Duc, Obinna Barah, Chidozie Ikpa, Francis Orji, George Alaneme, Ezenwa Amanamba, Henry Ugwuanyi, Vishnu Sai, Chukwuma Kadurumba, Selvakumar Subburaj and Benjamin Ugorji.** Recycling and reuse of solid wastes: A hub for ecofriendly, ecoefficient and sustainable soil, concrete, wastewater and pavement reengineering. International Journal of Low-Carbon Technologies vol. 14, 2019, pp. 440-451.

[49] **Wui Seng Ang, Ngai Yin Yip, Alberto Tiraferri and Menachem Elimelech.** Chemical cleaning of RO membranes fouled by wastewater effluent: Achieving higher efficiency with dual-step cleaning. Journal of Membrane Science, vol. 382, 2011, pp. 100-106.

[50] **Zehbah Ali Ahmed, Abeer Hassan, Sahar Khouly and Shaymaa El-Shafey.** TEMPO-oxidised cellulose nanofbers/TiO2 nanocomposite as new adsorbent for Brilliant Blue dye removal. Polymer Bulletin, vol. 77, 2020, pp. 6213-6226.

## List of Symbols and Abbreviations

| Symbol | Definition | Unit |
|---|---|---|
| **A** | Area | $m^2$ |
| **m** | Mass | g |
| **$C_{feed}$** | Concentration of feed solution | mmol/L |
| **$C_{permeate}$** | Concentration of the filtered solution | mmol/L |
| **G** | Coat weight/grammage | $g/m^2$ (= gsm) |
| **$G_{set}$** | Set coat weight | $g/m^2$ |
| **$G_{rcw}$** | Real coat weight | $g/m^2$ |
| **p** | Backpressure forcing deionised water through the filter | MPa |
| **P** | Permeance = volume of water passed through a filter per unit time, unit area and unit pressure | [$L/m^2$ h Mpa] |
| **$q_A$** | Areic adsorption = mass of adsorbed copper ions [mg] per unit filter area [$m^2$]. | $mg/m^2$ |
| **$q_e$** | Adsorption capacity, mass of copper per unit mass active adsorption agent | mg/g |
| **S** | Shrinkage of foam TEMPO-CNF coated filters during the drying process | - |
| **t** | Time to collect permeate fraction | s |
| **V** | Volume of permeate fraction collected | mL |
| **$V_{Titration}$** | Volume of solution that is titrated | mL |

| Abbreviations | |
|---|---|
| **BNC** | Bacterial nanocellulose |
| **CNF** | Cellulose nanofibril |
| **CNC** | Cellulose nanocrystal |
| **EDTA** | Ethylenediaminetetraacetic acid |
| **EMPA** | Swiss Federal Laboratories for Materials Science and Technology |
| **NC** | Nanocellulose |
| **NF** | Nanofiltration |
| **RO** | Reverse osmosis |
| **SEM** | Scanning electron microscopy |
| **SUTCO** | Surface Treatment Concept |
| **SWG** | Slot-web gap |
| **TEMPO** | 2,2,6,6-tetramethylpiperidin-1-oxyl |
| **UF** | Ultrafiltration |
| **VTT** | Technical Research Centre of Finland |

## List of Tables



## List of Figures